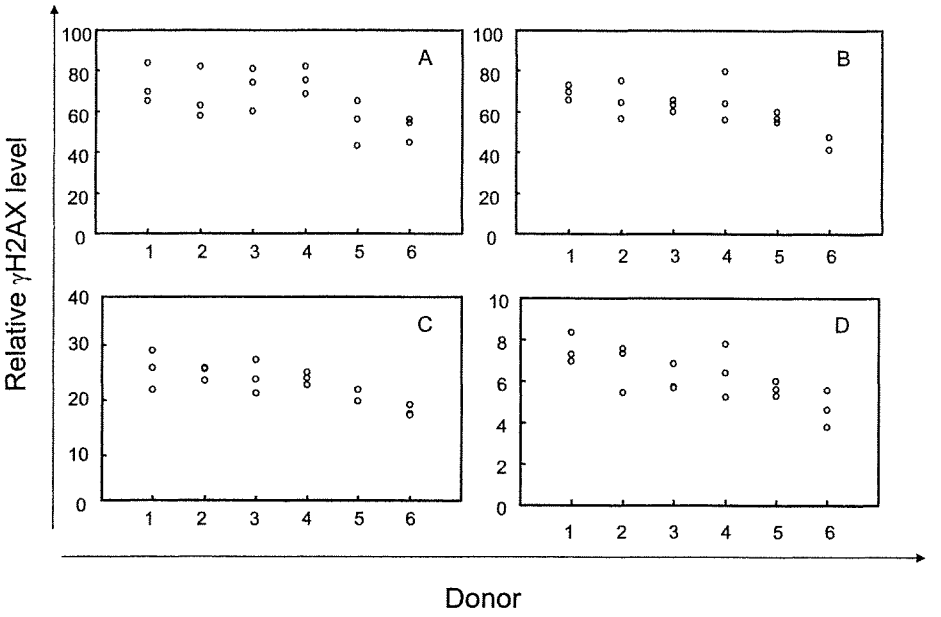


**Fig. 5.** Variability in the level of radiation-induced γH2AX among six healthy adults. Three independent experiments were carried out using T lymphocytes obtained from the same six individuals and cultured for 7 days before 4 Gy irradiation. Values obtained from the same experiment are plotted with the same symbols. Distributions of individual values for radiation-induced γH2AX level were analyzed for interindividual and interexperimental variation by one-way analysis of variance (ANOVA). (**A**) Relative γH2AX levels 1 hr after irradiation. Interindividual variability: $F = 8.46$; $P = 0.002$. Interexperimental variability: $F = 11.5$; $P = 0.003$. (**B**) The levels, 2 hr after irradiation. Interindividual variability: $F = 7.99$; $P = 0.003$. Interexperimental variability: $F = 3.13$; $P = 0.088$. (**C**) The levels 6 hr after irradiation. Interindividual variability: $F = 6.23$; $P = 0.007$. Interexperimental variability: $F = 1.64$; $P = 0.243$. (**D**) The levels 24 hr after irradiation. Interindividual variability: $F = 5.25$; $P = 0.013$. Interexperimental variability: $F = 3.64$; $P = 0.065$.

tion was significant, or marginally so, for 1 and 2 hr after irradiation, there was no significant interexperimental variation in the γH2AX level 6 hr after irradiation. These results suggest that for the assessment of individual radiation sensitivity relative to radiation-induced γH2AX levels, measurements tested at 6 hr after irradiation are the most reliable.

### Relationship Between γH2AX Level Measured by FCM and Number of γH2AX Foci Visualized by Microscopy

To ensure that the γH2AX level determined by FCM corresponded to the number of γH2AX foci in each cell, we sorted and collected three appropriate fractions showing different levels of γH2AX and counted by fluorescence microscopy the number of γH2AX foci per cell in each of the fractions collected. As shown in Figure 6, the level of γH2AX measured by FCM almost paralleled the mean number of γH2AX foci per cell in each fraction. Statistical analysis using the Jonckheere-Terpstra test indicated that there was a significant association between the values determined by these different assays ($P < 0.001$).

We also analyzed the number of γH2AX foci in irradiated cells of individuals with high and low T-cell radiosensitivity (Donors 2 and 6) and found that the γH2AX levels analyzed by FCM closely corresponded with the number of γH2AX foci observed microscopically (Fig. 7). Because the number of γH2AX foci represents the number of DSBs in irradiated cells [Rogakou et al., 1999] and positively correlates with radiosensitivity of the cells [MacPhail et al., 2003a], differences in the level of γH2AX expression 6 hr after irradiation may reflect the difference in unrepaired DSBs. It should be noted, however, that there was no indication of radiation-induced apoptosis in cultured T lymphocytes within this 6 hr postirradiation time-frame (data not shown). This suggests that the radiation-induced γH2AX expression detected in the present study by either FCM or by microscopy probably does not involve apoptosis-related events resulting from radiation exposure.

### Lymphocyte Subsets and Radiation-Induced γH2AX Levels

To characterize more fully the lymphocyte pools used in the FCM-γH2AX assays, we determined the percentages of lymphocyte subsets (CD3, CD4, CD8, CD16, and CD20) before and 7 days after culture for the six individuals we studied. The cell population just before irradiation was mainly composed of CD4 (10–40%) and CD8 (60–80%) T-cell populations, and a majority of these T-cell populations expressed a low level of CD45RA, a memory-phenotype indication. Other lymphocyte populations,

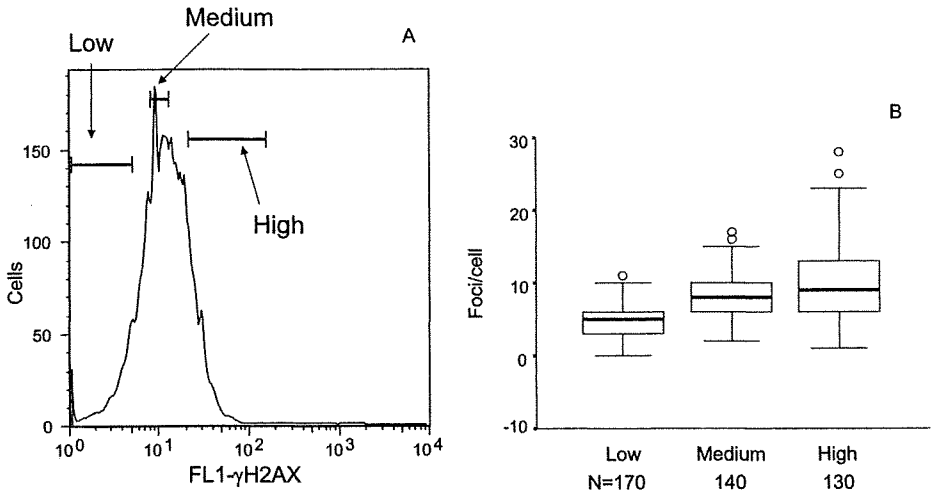


**Fig. 6.** Associations between γH2AX levels measured with FCM and the number of γH2AX foci determined by fluorescence microscopy in irradiated cultured T-lymphocyte fractions from one individual (Donor 2). (**A**) Each cell fraction showing low (1–5 fluorescence channels), medium (8–13 fluorescence channels), or high (21–160 fluorescence channels) γH2AX fluorescence intensities was sorted from cultured T lymphocytes obtained from one individual and stained for γH2AX expression 6 hr after 2 Gy irradiation. (**B**) Box plots of the number of foci per cell in each cell fraction. Totally 130–170 cells for each fraction were analyzed by fluorescence microscopy using Image Pro Plus 4.5 software. The horizontal line in each of the middle of boxes marks the median value in each fraction. The lower and upper edges of each box mark the 25th and 75th percentiles, respectively, and thus the central 50% of the data values fall within the range of the box. The vertical lines extending up and down from each box show the largest and the smallest values observed, respectively, and open circles mark the "outside values," which are between 1.5- and 3.0-times higher than the 75th percentile values. The Jonckheere-Terpstra test indicated that there was a significant association between γH2AX levels measured with FCM and the number of γH2AX foci determined by fluorescence microscopy ($P < 0.001$).

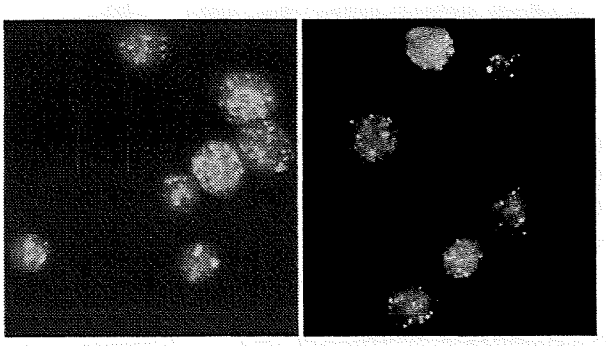

| | Donor 2 | Donor 6 |
|---|---|---|
| Number of foci | 1085 | 1082 |
| Cells analyzed | 117 | 147 |
| Average (foci / cell) ± SD | 9.3 ± 5.6 | 7.4 ± 4.9 |

$p < 0.004$

**Fig. 7.** Fluorescence microscopy analysis of γH2AX foci in cultured T lymphocytes from two individuals (Donors 2 and 6). The number of foci in cells was analyzed 6 hr after 4 Gy irradiation using Image Pro Plus 4.5 software. The average number of γH2AX foci per cell differed significantly between these two individuals ($P = 0.004$, the Students' *t*-test).

namely B and NK cells, were quite small (less than 3%). There was no obvious relationship between levels of radiation-induced γH2AX in individuals and percentages of lymphocyte subsets either before or after cell culture (data not shown). To further support the idea that differences in the CD4 and CD8 T-cell ratio does not contribute to individual differences in radiation-induced γH2AX expression, we analyzed γH2AX levels in separately cultured and irradiated CD4 and CD8 T-cell fractions from Donors 2 and 6. There was no obvious difference in the levels of radiation-induced γH2AX between CD4 and CD8 T-cell subsets in the same individuals. Difference between these individuals in terms of these subsets were apparent, i.e., γH2AX levels in CD4 and CD8 T-cell sub-

sets of Donor 2, 6 hr after 4 Gy irradiation were 32.0 and 28.7, respectively, whereas those in the comparable subsets of Donor 6 were 26.4 and 24.3, respectively. These results suggest that the differences in radiation-induced γH2AX levels in cultured T lymphocytes between individuals are not related to differences in the proportion of lymphocyte subsets within the test samples.

## DISCUSSION

In this study, we established an FCM system for measuring levels of radiation-induced γH2AX in human lymphocytes to assess individual differences in radiation sensitivity to DNA damage in vitro. Currently, γH2AX focus formation is being used as a DNA damage marker, specifically for DSBs induced by exposure to various genotoxic agents, such as ionizing radiation [Rogakou et al., 1999]. γH2AX recruits other enzymes related to the DNA repair process (such as 53BP1, BRCA1, the NBS/MRE11/RAD50 complex), and thereby plays a key role in early phases of the repair of damaged cells [Paull et al., 2000; Celeste et al., 2002, 2003; Kobayashi, 2004]. We thought that by measuring cellular levels of γH2AX by high-throughput FCM, a rapid and accurate assessment of radiation sensitivity in human individuals might be possible. It has been reported that the background γH2AX level in normal cells differs at each phase of the cell cycle and appears particularly high at the S to G2/M phases [Ichijima et al., 2005; McManus and Hendzel, 2005]. Our FCM system can analyze radiation-induced γH2AX levels in cells at each phase of the cell cycle, which has been very difficult using conventional fluorescence microscopy analysis. Therefore, one major advantage of our method is that G1-phase cells, with low background γH2AX levels, can be selectively targeted for analyses.

We expect that the γH2AX FCM system established in this study will allow straightforward assessments of both individual sensitivity to radiation-induced DNA damage and individual ability to repair such DNA damage. By applying γH2AX FCM to an epidemiological follow-up study cohort, such as the A-bomb survivor populations in Hiroshima and Nagasaki, we will be able to address the important question of whether or not individuals who have lower DNA repair ability have higher mutability in response to radiation, and in turn, higher risks of radiation-related cancers.

In this study, radiation-induced γH2AX levels in blood lymphocytes appeared to be about 1.5-fold higher if the cells were cultured for 7 days prior to radiation exposure (Fig. 2). It is highly likely that growth-stimulated T lymphocytes (via PHA and IL-2) were more severely damaged by ionizing radiation than were resting peripheral blood lymphocytes. This is consistent with an earlier finding of 20-fold increases in DNA repair synthesis following ionizing irradiation of stimulated lymphocytes compared with resting lymphocytes [Lavin and Kidson, 1977]. However, it is unclear why individual differences in radiation-induced γH2AX levels can be detected more readily in cultured T lymphocytes than in freshly isolated and resting lymphocytes. This partly may be due to the relatively low γH2AX levels within resting irradiated lymphocytes that have not been growth-activated in vitro and the substantial differences in metabolic status between cultured and uncultured lymphocytes, such as specific variations in activities of DNA repair enzymes. However, it has been previously reported that the transcriptional levels of most DNA repair genes were not significantly increased in PHA-stimulated lymphocytes when compared with levels in resting lymphocytes [Mayer et al., 2002]. Therefore, it is unlikely that differences in the activity of DNA repair genes are the cause of individual differences in residual γH2AX levels in irradiated cultured T lymphocytes. Alternatively, differences in radiation sensitivity between cultured and uncultured T lymphocytes might result from differences in the ability of irradiated cells to scavenge DNA-damaging radicals induced by ionizing radiation. Further testing is required regarding whether the genes responsible for radical scavenger proteins are substantially upregulated in cultured T lymphocytes, and whether there are differences in levels of these proteins in cultured T lymphocytes from different individuals.

Differences in individual radiosensitivity were not as obvious in T lymphocytes cultured for 13 days (Fig. 4). Previously, it had been shown that the cell growth rate declined appreciably in similar T-cell cultures 10–14 days after the beginning of culture [Ishioka et al., 1997]. This decline may have been simply due to growth arrest mediated by attenuated T-cell receptor and/or growth factor signals. Simply stated, the diminished responses were probably the result of the cultured T lymphocytes being in a resting state at the time of testing (13th day).

γH2AX levels detected with FCM in a given fraction of irradiated T lymphocytes were able to fully reflect the mean number of microscopically detected γH2AX foci per cell in the same fraction (Fig. 6). It is probable that the γH2AX detected by FCM was related to the levels of radiation-induced DSBs in the same fraction as well. It is therefore likely that individual differences observed in γH2AX-FCM are related to differences in the degree of DNA damage and in the individual's ability to repair DNA damage.

In this study, there was no obvious difference in radiation-induced γH2AX levels between CD4 and CD8 T-cell populations obtained and cultured from the same individuals. Our previous study [Nakamura et al., 1990] showed that survival fractions after in vitro irradiation did not differ significantly between these subsets when they were isolated from the same individuals and irradiated before

culture with PHA and IL-2. Radiation-induced micronucleus frequencies also were similar among peripheral T-cell subpopulations [Ban and Cologne, 1992]. Therefore, it is likely that CD4 and CD8 T lymphocytes, which comprise the majority of peripheral blood T lymphocytes, exhibit comparable radiation sensitivities independent of their activation. Moreover, the cultured T-lymphocyte populations used in the present study for individual radiation sensitivity appeared to be mainly composed of memory T-lymphocytes, with more than half memory CD8 T-lymphocytes. It has been reported that memory T-lymphocytes are more radiation-sensitive than naïve T lymphocytes [Uzawa et al., 1994]. Therefore, it is possible that excessive proliferation of memory CD8 T-lymphocytes in the culture might affect the individual radiosensitivity difference that we detected with γH2AX-FCM. However, it is unlikely that the differences in the percentages of memory CD8 T-lymphocytes in the tested cell samples were related to the individual variability in radiation-induced γH2AX levels (data not shown). Accordingly, we believe that these relatively small differences in the proportion of T-lymphocyte subpopulations do not significantly influence the γH2AX-FCM testing procedures that we described for evaluating radiation sensitivity in vitro.

## ACKNOWLEDGMENTS

The authors are grateful to Drs. Tomonori Hayashi, Seishi Kyoizumi, Asao Noda, Charles A. Waldren, and Thomas M. Seed for their helpful advice. They also would like to thank Mika Yamaoka and Yoshiko Kubo for their excellent assistance regarding the use of FCM.

The Radiation Effects Research Foundation (RERF), Hiroshima and Nagasaki, is a private nonprofit foundation funded by the Japanese Ministry of Health, Labour and Welfare, and the United States Department of Energy, the latter through the National Academy of Sciences. This publication was based on RERF Research Protocol RP 3-87.

## REFERENCES

Ban S, Cologne JB. 1992. X-ray induction of micronuclei in human lymphocyte subpopulations differentiated by immunoperoxidase staining. Radiat Res 131:60–65.

Banath JP, Macphail SH, Olive PL. 2004. Radiation sensitivity, H2AX phosphorylation, and kinetics of repair of DNA strand breaks in irradiated cervical cancer cell lines. Cancer Res 64:7144–7149.

Celeste A, Petersen S, Romanienko PJ, Fernandez-Capetillo O, Chen HT, Sedelnikova OA, Reina-San-Martin B, Coppola V, Meffre E, Difilippantonio MJ, Redon C, Pilch DR, Olaru A, Eckhaus M, Camerini-Otero RD, Tessarollo L, Livak F, Manova K, Bonner WM, Nussenzweig MC, Nussenzweig A. 2002. Genomic instability in mice lacking histone H2AX. Science 296:922–927.

Celeste A, Fernandez-Capetillo O, Kruhlak MJ, Pilch DR, Staudt DW, Lee A, Bonner RF, Bonner WM, Nussenzweig A. 2003. Histone H2AX phosphorylation is dispensable for the initial recognition of DNA breaks. Nat Cell Biol 5:675–679.

Hagmar L, Stromberg U, Bonassi S, Hansteen IL, Knudsen LE, Lindholm C, Norppa H. 2004. Impact of types of lymphocyte chromosomal aberrations on human cancer risk: Results from Nordic and Italian cohorts. Cancer Res 64:2258–2263.

Ichijima Y, Sakasai R, Okita N, Asahina K, Mizutani S, Teraoka H. 2005. Phosphorylation of histone H2AX at M phase in human cells without DNA damage response. Biochem Biophys Res Commun 336:807–812.

Ishioka N, Umeki S, Hirai Y, Akiyama M, Kodama T, Ohama K, Kyoizumi S. 1997. Stimulated rapid expression in vitro for early detection of in vivo T-cell receptor mutations induced by radiation exposure. Mutat Res 390:269–282.

Kobayashi J. 2004. Molecular mechanism of the recruitment of NBS1/hMRE11/hRAD50 complex to DNA double-strand breaks: NBS1 binds to γ-H2AX through FHA/BRCT domain. J Radiat Res (Tokyo) 45:473–478.

Kushiro J, Hirai Y, Kusunoki Y, Kyoizumi S, Kodama Y, Wakisaka A, Jeffreys A, Cologne JB, Dohi K, Nakamura N, Akiyama M. 1992. Development of a flow-cytometric HLA-A locus mutation assay for human peripheral blood lymphocytes. Mutat Res 272:17–29.

Kusunoki Y, Kodama Y, Hirai Y, Kyoizumi S, Nakamura N, Akiyama M. 1995. Cytogenetic and immunologic identification of clonal expansion of stem cells into T,B lymphocytes in one atomic-bomb survivor. Blood 86:2106–2112.

Kusunoki Y, Kyoizumi S, Hirai Y, Suzuki T, Nakashima E, Kodama K, Seyama T. 1998. Flow cytometry measurements of subsets of T,B and NK cells in peripheral blood lymphocytes of atomic bomb survivors. Radiat Res 150:227–236.

Lavin MF, Kidson C. 1977. Repair of ionizing radiation induced DNA damage in human lymphocytes. Nucleic Acids Res 4:4015–4022.

MacPhail SH, Banath JP, Yu TY, Chu EH, Lambur H, Olive PL. 2003a. Expression of phosphorylated histone H2AX in cultured cell lines following exposure to X-rays. Int J Radiat Biol 79:351–358.

MacPhail SH, Banath JP, Yu Y, Chu E, Olive PL. 2003b. Cell cycle-dependent expression of phosphorylated histone H2AX: Reduced expression in unirradiated but not X-irradiated G1-phase cells. Radiat Res 159:759–767.

Mayer C, Popanda O, Zelezny O, von Brevern MC, Bach A, Bartsch H, Schmezer P. 2002. DNA repair capacity after γ-irradiation and expression profiles of DNA repair genes in resting and proliferating human peripheral blood lymphocytes. DNA Repair (Amst) 1:237–250.

McManus KJ, Hendzel MJ. 2005. ATM-dependent DNA damage-independent mitotic phosphorylation of H2AX in normally growing mammalian cells. Mol Biol Cell 16:5013–5025.

Mukherjee B, Kessinger C, Kobayashi J, Chen BP, Chen DJ, Chatterjee A, Burma S. 2006. DNA-PK phosphorylates histone H2AX during apoptotic DNA fragmentation in mammalian cells. DNA Repair (Amst) 5:575–590.

Nakamura N, Kusunoki Y, Akiyama M. 1990. Radiosensitivity of CD4 or CD8 positive human T-lymphocytes by an in vitro colony formation assay. Radiat Res 123:224–227.

Ohara M, Hayashi T, Kusunoki Y, Miyauchi M, Takata T, Sugai M. 2004. Caspase-2 and caspase-7 are involved in cytolethal distending toxin-induced apoptosis in Jurkat and MOLT-4 T-cell lines. Infect Immun 72:871–879.

Parshad R, Price FM, Bohr VA, Cowans KH, Zujewski JA, Sanford KK. 1996. Deficient DNA repair capacity, a predisposing factor in breast cancer. Br J Cancer 74:1–5.

Paull TT, Rogakou EP, Yamazaki V, Kirchgessner CU, Gellert M, Bonner WM. 2000. A critical role for histone H2AX in recruitment of repair factors to nuclear foci after DNA damage. Curr Biol 10:886–895.

Roberts SA, Spreadborough AR, Bulman B, Barber JB, Evans DG, Scott D. 1999. Heritability of cellular radiosensitivity: A marker of low-penetrance predisposition genes in breast cancer? Am J Hum Genet 65:784–794.

Rogakou EP, Pilch DR, Orr AH, Ivanova VS, Bonner WM. 1998. DNA double-stranded breaks induce histone H2AX phosphorylation on serine 139. J Biol Chem 273:5858–5868.

Rogakou EP, Boon C, Redon C, Bonner WM. 1999. Megabase chromatin domains involved in DNA double-strand breaks in vivo. J Cell Biol 146:905–916.

Scott D, Barber JB, Levine EL, Burrill W, Roberts SA. 1998. Radiation-induced micronucleus induction in lymphocytes identifies a high frequency of radiosensitive cases among breast cancer patients: A test for predisposition? Br J Cancer 77:614–620.

Scott D, Barber JB, Spreadborough AR, Burrill W, Roberts SA. 1999. Increased chromosomal radiosensitivity in breast cancer patients: A comparison of two assays. Int J Radiat Biol 75: 1–10.

Takahashi A, Ohnishi T. 2005. Does γH2AX foci formation depend on the presence of DNA double strand breaks? Cancer Lett 229: 171–179.

Terzoudi GI, Jung T, Hain J, Vrouvas J, Margaritis K, Donta-Bakoyianni C, Makropoulos V, Angelakis P, Pantelias GE. 2000. Increased G2 chromosomal radiosensitivity in cancer patients: The role of cdk1/cyclin-B activity level in the mechanisms involved. Int J Radiat Biol 76:607–615.

Uzawa A, Suzuki G, Nakata Y, Akashi M, Ohyama H, Akanuma A. 1994. Radiosensitivity of CD45RO+ memory and CD45RO− naive T cells in culture. Radiat Res 137:25–33.

West CM, Davidson SE, Elyan SA, Valentine H, Roberts SA, Swindell R, Hunter RD. 2001. Lymphocyte radiosensitivity is a significant prognostic factor for morbidity in carcinoma of the cervix. Int J Radiat Oncol Biol Phys 51:10–15.

*Accepted by*—
W. F. Morgan

*Report*

# Radiation sensitivity and genomic instability in the hematopoietic system: Frequencies of micronucleated reticulocytes in whole-body X-irradiated BALB/c and C57BL/6 mice

**Kanya Hamasaki, Kazue Imai, Tomonori Hayashi, Kei Nakachi and Yoichiro Kusunoki[1]**

Department of Radiobiology/Molecular Epidemiology, Radiation Effects Research Foundation, 5-2 Hijiyama Park, Minami-ku, Hiroshima 732-0815, Japan

(Received June 4, 2007/Revised August 6, 2007/2nd Revision August 13, 2007/Accepted August 19, 2007/Online publication October 9, 2007)

**Using flow cytometry, we quantified the number of micronucleated reticulocytes in peripheral blood of whole-body X-irradiated mice in order to evaluate the radiation sensitivity and the induced genomic instability of the hematopoietic system. An acute effect of radiation dose as small as 0.1 Gy was detectable 2 days after irradiation, and the radiation dose effect was significantly greater in BALB/c mice than in C57BL/6 mice, that is, 3.0- and 2.3-fold increases in frequencies of micronuclei were noted in the two groups of mice, respectively. Even 1 year after irradiation, mice irradiated with 2.5 Gy of X-rays showed significantly increased frequencies of micronucleated reticulocytes, that is, 1.6- and 1.3-fold increases in BALB/c and C57BL/6 mice, respectively. However, this delayed effect was not apparent when the same mice were analyzed for T-cell receptor mutant frequencies in splenocytes. A significant mouse strain difference in the delayed radiation effect on micronucleated reticulocyte frequencies was noted as well. The results indicate that delayed genomic effects of irradiation on the murine hematopoietic system can persist *in vivo* for prolonged periods, and that there are mouse strain differences in sensitivity to radiation-induced genomic instability. (*Cancer Sci* 2007; 98: 1840–1844)**

Chromosome aberrations and gene mutations directly induced by ionizing radiation in hematopoietic stem cell populations were conventionally thought to be causative molecular mechanisms of radiation leukemogenesis. However, recent studies have shown that comparable genomic alterations can occur in unirradiated cells that either lie adjacent to irradiated cells or are the descendants of irradiated cells. Such indirect radiation effects reflect radiation-induced genomic instabilities, and are thought to represent adverse cellular responses that can lead to malignant transformation.[1] Although radiation-induced genomic instability is well characterized *in vitro* by the delayed appearance of specific types of genomic damage (e.g. chromosomal aberrations, gene mutations) in the progeny of irradiated cells, evidence from *in vivo* studies has been limited due to the lack of reliable bioassays that are capable of detecting delayed genomic alterations induced by irradiation in large cell populations in an objective and straightforward manner. Previous reports on radiation-induced genomic instability *in vivo* have been somewhat contradictory: one reported study showed that chromosomal instability induced in normal hematopoietic cells was maintained for a prolonged period *in vivo*,[2] whereas another report showed no such detectable chromosomal instability in hematopoietic cells of irradiated mice.[3] It has been suggested that susceptibility to radiation-induced genomic instability might be dependent on genetic factors, at least in mice, that is, strain differences in experimental mice.[4]

*In vivo* rodent erythrocyte micronucleus (MN) assays are widely used to evaluate the genotoxic effects of chemical and physical agents, and several high throughput methods using flow cytometry for micronucleated reticulocyte enumeration developed.[5–7] The principle of MN assay is that portion(s) of chromosome(s) remain in the cell when the erythroblast extrudes the nucleus during the final stage of maturation to become a nearly mature reticulocyte. These fragments are easily enumerated, as are reticulocytes, by flow cytometry using a combination of fluorescence dyes (such as propidium iodide) that bind to DNA, and reticulocyte cell markers (such as transferrin receptor CD71). Because the estimated lifespan of reticulocytes *in vivo* is as short as a few days,[8] reticulocyte MN observed more than 1 month after irradiation is not the consequence of direct radiation damage to these cells, but rather is due to indirect damage resulting from radiation-induced genomic instabilities with precursor cells with damage manifested during this course of normal erythropoiesis. As such, this process allowed us to analyze delayed radiation effects separately from direct ones.

In the present study, we analyzed both acute and delayed effects of ionizing radiation on reticulocyte MN frequencies in whole-body X-irradiated BALB/c and C57BL/6 mice. We also measured frequencies of TCR mutant splenic CD4 T cells[9] among these irradiated mice, to investigate mutability at a specific gene locus among mice to which genomic instability has possibly been induced. Our results showed that MN frequencies, but not TCR mutant frequencies, were significantly increased in these mice, even 1 year after irradiation with moderately low doses of 2.5 Gy. It also appeared that there were differences in sensitivities between mouse strains in terms of radiation-induced genomic instability assessed by MN frequencies.

## Materials and Methods

**Mice.** Female C57BL/6 and BALB/c mice were purchased from Japan Clea Co. (Tokyo, Japan). All mice were housed in autoclaved microisolator cages and fed a sterile regular diet *ad libitum*. All animal handling procedures were approved by the Experimental Animal Care Committee of the Radiation Effects

[1]To whom correspondence should be addressed. E-mail: ykusunok@rerf.or.jp
Abbreviations: MN, micronucleus; TCR, T-cell receptor.



doi: 10.1111/j.1349-7006.2007.00641.x

Research Foundation. The mice were X-irradiated (220 kVp, 8 mA, 0.7 Gy/min) at 10 weeks of age.

**Reticulocyte MN assay.** One hundred to 200 microliters of blood was obtained from ether-anesthetized mice by orbital sinus bleeding, and analyzed by flow cytometry using the mouse MN analysis kit MicroFlow$^{PLUS}$ Kit (mouse) (Litron Laboratories, Rochester, NY), according to the manufacturer's instructions. Briefly, the blood was mixed with 350 μL of the anticoagulant solution supplied in the kit, and a 180 μL aliquot of the diluted blood was fixed with 2 mL of –80°C absolute methanol and kept in an ultracold (–75 to –85°C) freezer. After washing the fixed cells, 20 μL aliquots of each cell pellet were added to tubes containing fluorescein-labeled anti-CD71 and phycoerythrin-labeled anti-CD61 antibodies and RNase A to differentially stained erythrocyte cell populations. One milliliter of cold propidium iodide solution was then added to labeled MN, and the stained cells were subsequently analyzed quantitatively by a FACScan flow cytometer (BD Biosciences, Franklin Lakes, NJ). More than 20 000 reticulocytes gated on $CD71^+/CD61^-$ populations were analyzed to determine MN frequencies. Data analysis was carried out using FlowJo software (Tree Star, Ashland, OR).

**TCR mutant assay.** TCR mutant frequencies were determined using a flow cytometry assay previously established in our laboratory,[9] with some modifications. In brief, $3 \times 10^6$ splenocytes were stained with 20 μL of phycoerythrin-labeled anti-CD3∈ antibody (BD Biosciences), 10 μL of phycoerythrin-labeled anti-I-A/I-E antibody (BD Biosciences), and 20 μL of fluorescein-labeled anti-CD4 antibody (Caltag Laboratories, San Francisco, CA) and examined with a FACScan. TCR mutants were detected as cells expressing CD4 but lacking CD3. TCR mutant frequencies were expressed as ratios of the numbers of mutants in test samples to the total numbers of CD4 T cells in the same samples. Nylon-wool-adherent cells, which might contaminate the mutant fraction,[9] were completely excluded from the $CD4^+CD3^-$ mutant population according to their I-A/I-E positive phenotype in the flow cytometry (data not shown).

**Statistical analysis.** SPSS version 14.0 software (SPSS, Chicago, IL) was used for statistical analyses. Effects of radiation and *P*-trends were analyzed by Mann–Whitney and Jonckheere–Terpstra tests, respectively. Mouse strain difference in the slope for linear dose–response of MN frequency was examined by *t*-test.

## Results and Discussion

Consistent with an earlier study,[10] MN frequencies in C57BL/6 mice periodically measured after whole-body irradiation with 2.5 Gy of X-rays appeared to reach a peak on the second day (data not shown). Therefore, radiation dose effects were analyzed on the second day postirradiation in both C57BL/6 and BALB/c mice. Typical flow cytometry patterns are shown in Fig. 1a, using C57BL/6 mice exposed to 0.0, 0.1, or 0.5 Gy. Significant radiation dose-dependent responses were found in both C57BL/6 and BALB/c mice (Fig. 1b,c, respectively, $P$-trend < 0.001). Furthermore, significant effects from radiation doses as small as 0.1 Gy were detected in C57BL/6 mice (2.3 times higher than controls, $P = 0.002$) as well as in BALB/c mice (3.0 times higher than controls, $P = 0.002$), with the dose–response lower in the former than in the latter ($P < 0.001$, C57BL/6 *versus* BALB/c) (Fig. 1b,c). This noted mouse strain difference in sensitivity to radiation-induced genomic damage is similar to our previous findings on the frequencies of TCR mutant cells in such mice.[9]

To determine whether or not the radiation-induced genomic instability of the mouse hematopoietic system was detectable even 1 year after irradiation, we measured MN frequencies in mice that had been irradiated with 2.5 Gy of X-rays 1 year earlier, and compared those frequencies with MN frequencies in age-matched controls (Fig. 2). Average MN frequencies in the irradiated C57BL/6 and BALB/c mice were 0.13% and 0.19%, respectively, that is, 1.3- and 1.6-fold higher than those in the controls ($P = 0.039$ and $P = 0.035$, respectively). Although this delayed radiation effect was smaller than the acute effect in those exposed to 0.1 Gy, Fig. 2 clearly indicates that there is long-lasting genomic instability in the hematopoietic system of mice exposed to ionizing radiation. Of note was the significant difference between mouse strains in the delayed radiation effect ($P = 0.028$). This result is consistent with previous findings of delayed radiation effects on chromosome aberrations in irradiated and cultured epithelial cells from BALB/c mice, but not in cells from C57BL/6 mice.[11] Such resistance to radiation-induced chromosomal instability is also known for hematopoietic cell populations in C57BL/6 mice.[4] The discrepancy between those chromosome studies and our findings might be due, at least partly, to the considerably low level of genomic instability induced by irradiation in the mice in our study. That is, the 1.3-fold increase in the frequency of genomic damage that we observed by flow cytometry might be undetectable by conventional cytogenetic analyses.

In the same mice for which reticulocyte MN frequencies were evaluated 1 year after 2.5 Gy of X-irradiation, we also examined frequencies of TCR mutants to investigate whether we could observe any significant changes in mutation frequencies at a specific gene locus of mice to which genomic instability was possibly induced. Because the half-life of radiation-induced TCR mutants in mice was estimated to be approximately 2 weeks,[9] and because the target of TCR mutations was assumed to be the mature T-cell population that completed TCR gene rearrangements in the thymus,[9] we also expected to detect elevated TCR mutant frequencies in the irradiated mice if genomic instability was induced into the peripheral T-cell systems of these mice. However, there was no significant difference in TCR mutant frequencies between irradiated and control mice in either the C57BL/6 or BALB/c strain (Fig. 2c,d). Average TCR mutant frequencies in the irradiated C57BL/6 and BALB/c mice were $4.6 \times 10^{-4}$ and $4.5 \times 10^{-4}$, respectively, that is, 1.2- and 1.3-fold higher than those in the controls ($P = 0.097$ and $P = 0.32$, respectively). There are at least two possibilities that can explain why we failed in the detection of radiation-induced genomic instability in the T-cell system. One is that the sensitivity of the TCR mutation assay was not high enough to detect such 1.3–1.6 fold increases as could be detected by the reticulocyte MN assay. Whereas an acute dose effect of 0.5 Gy could not be detected by the TCR mutation assay (data not shown), the effect of as few as 0.1 Gy could be detected by the reticulocyte MN assay (Fig. 1). Such a discrepancy in detection sensitivity might result from the difference in measurement endpoints between these two assays, that is, the TCR mutation assay enumerates cells lacking specific gene expression, and the reticulocyte MN assay counts cells with aberrant chromosomes. In other words, the latter assay might more directly, and hence more reliably, evaluate genomic damage in the hematopoietic system than the former. The other possibility is that mature T cells that were genetically instable and therefore assumed to produce a number of mutant progenies might have been eliminated effectively in the process of maintaining T-cell homeostasis. It is known that the maintenance of T-cell homeostasis is largely, but not entirely, accomplished by replication and death of mature T cells.[12]

Numerous studies have shown that the frequency of genomic damage in somatic cells generally increases with age (reviewed by Morley).[13] In the present study, however, there was no obvious difference in MN frequencies between unirradiated young and aged mice; average MN frequencies in the unirradiated C57BL/6 and BALB/c mice at 10 weeks of age were 0.11% and

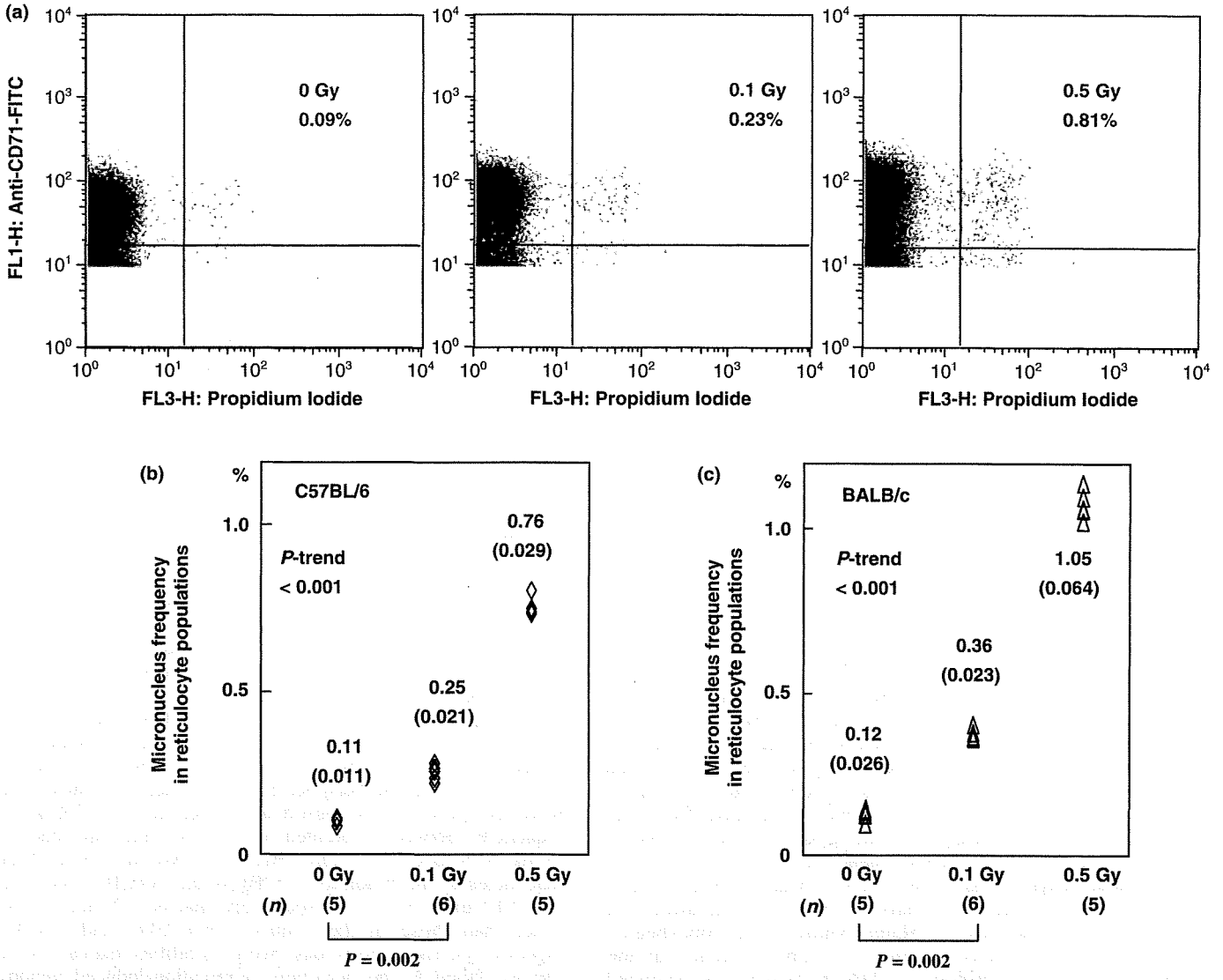


**Fig. 1.** Flow cytometry analysis of reticulocyte micronucleus (MN) frequencies in mice 2 days after whole-body irradiation. (a) Typical flow cytometry patterns in C57BL/6 mice irradiated with 0.0, 0.1, and 0.5 Gy. (b, c) Radiation dose–responses of reticulocyte MN frequencies in C57BL/6 and BALB/c mice, respectively. The numbers in the vicinity of the symbols denote the mean and standard deviation, and those in parentheses at the bottom of each panel denote the number (*n*) of mice used in each group. Estimated linear dose–response for C57BL/6 mice is: MN frequency (%) = 0.12 (95% confident interval: 0.10, 0.13) + 1.28 (1.23, 1.40) × dose (Gy); for BALB/c mice: MN frequency (%) = 0.15 (0.11, 0.18) + 1.82 (1.70, 1.94) × dose (Gy). The regression coefficient (*r*) in each linear dose–response exceeds 0.99 and the slope for linear dose–response significantly differs between C57BL/6 and BALB/c mice ($P < 0.001$).

0.12%, respectively (Fig. 1b,c), and those in the unirradiated C57BL/6 and BALB/c mice at 1 year of age were 0.10% and 0.12%, respectively (Fig. 2a,b). The results are consistent with a previous study,[14] in which an age effect on reticulocyte MN frequencies was not significant in C57BL/6 mice at 38 weeks of age (being comparable to our study period). Our concurrently age-matched setting for irradiated and control mice excluded the possibility that the 1.3–1.6-fold increases of MN frequencies in the irradiated aged mice are reflections of the effects of aging.

The MN frequencies we detected *in vivo* 1 year after irradiation appeared to be somewhat lower than those previously reported in *in vitro* studies.[15] This difference might be due largely to the host defense mechanisms that effectively eliminate genetically damaged cells, or perhaps to differences in the mouse species/strains and/or cell lineages examined. In the present study, delayed MN formation was apparent in cells that were not directly targeted by radiation. Two scenarios, not mutually exclusive, could be implicated in this delayed radiation effect: (i) cells not directly irradiated but descended from irradiated cells showed genomic instability; and (ii) some mediators released from irradiated cells enhanced DNA damage in non-irradiated adjacent cells at the time of irradiation (bystander effects).[1,16] In the former scenario, genomic instability might have been induced in a portion of stem cells by genetic and/or epigenetic alteration(s) of one or more critical genes controlling genome integrity. Reactive oxygen species and inflammatory cytokines are possible mediators of bystander effects, and low-grade, chronic inflammation has been suggested to occur in atomic bomb survivors.[17] The latter scenario is plausible, but only if radiation-induced inflammation can cause elevated MN frequencies *in vivo*. Mutagenic effects of tumor necrosis factor-α have recently been reported,[18] in keeping with this line of reasoning. Further studies are necessary, however, to fully develop and understand the nature and consequences of radiation-induced genomic instability within the hematopoietic system.



doi: 10.1111/j.1349-7006.2007.00641.x

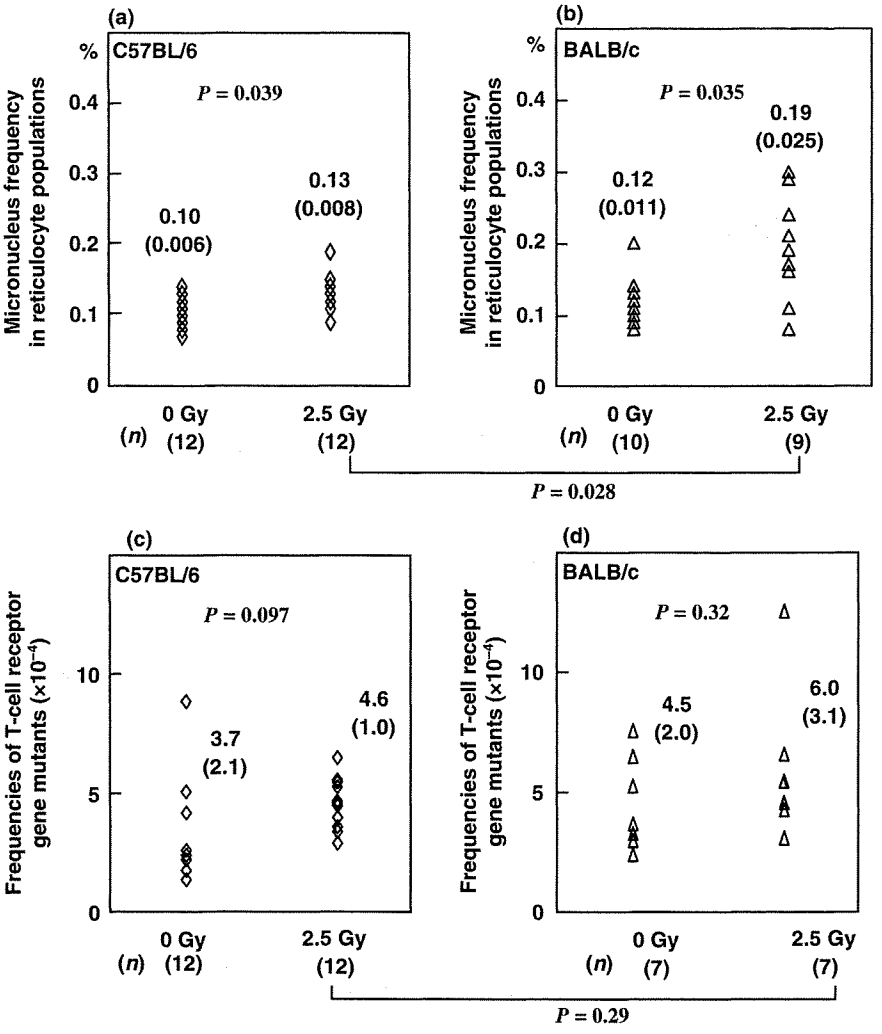


**Fig. 2.** Reticulocyte micronucleus (MN) frequencies (a, b) and frequencies of T-cell receptor (TCR) mutants (c, d) in C57BL/6 (a, c) and BALB/c (b, d) mice irradiated with 2.5 Gy of X-rays 1 year previously and in concurrent age-matched controls. Twelve irradiated and 13 unirradiated C57BL/6 mice were concurrently housed and analyzed under the same conditions. Of these, one unirradiated mouse had myeloid leukemia and was eliminated from MN analysis. Eleven irradiated and 11 unirradiated BALB/c mice were similarly housed and analyzed, and of these one unirradiated mouse with splenocytoma and two irradiated mice with ovarian cancer and lymphoma were eliminated from the MN analysis. Among the mice analyzed for MN frequencies, 12 irradiated and 12 unirradiated C57BL/6 mice and seven irradiated and seven unirradiated BALB/c mice were successfully analyzed for TCR mutant frequencies. The numbers above the symbols denote the mean and standard deviation, and those in parentheses at the bottom of each panel denote the number (*n*) of mice used in each group.

Although the mechanism of radiation carcinogenesis is still unknown, it is widely accepted that the accumulation of genomic damage in a target cell is required for the development of solid cancer as well as leukemia.[19,20] It is also proposed that genomic instability observed in the hematopoietic system of irradiated mice is very likely to be involved in the development of acute leukemia.[21] In atomic bomb survivors, the incidence of leukemia peaked within 10 years after exposure, and declined thereafter; whereas the excess risk of solid cancers started to increase approximately 20 years after the bombings, and continued to increase with time.[22] Frequent somatic mutations at the *AML1* gene have recently been suggested as the cause of myelodysplastic syndrome in survivors.[23] Our cancer follow-up study relating to mutations at the glycophorin A locus in erythrocytes among Hiroshima survivors also suggests that there might be interindividual variation in mutability of somatic genes and that those who have higher mutability in response to radiation exposure might have a higher probability of developing radiation-related cancer.[24] It is expected that evaluation of reticulocyte MN frequencies among people exposed to genotoxic agents such as radiation can provide a useful endpoint for estimation of individual risk of radiation-related malignancies.

## Acknowledgments

The authors are grateful to Mika Yamaoka and Yoshiko Kubo for their excellent assistance regarding use of flow cytometry. We also thank Makiko Hamamura for help with animal care.

The Radiation Effects Research Foundation, Hiroshima and Nagasaki, is a private non-profit foundation funded by the Japanese Ministry of Health, Labour and Welfare and the United States Department of Energy, the latter through the National Academy of Sciences. This publication was based on Radiation Effects Research Foundation Research Protocol RP 7-89 and RP 4-02, and supported in part by Grants-in-Aid for Scientific Research from the Japanese Ministry of Health, Labour and Welfare.

## References

1 Lorimore SA, Coates PJ, Wright EG. Radiation-induced genomic instability and bystander effects: inter-related nontargeted effects of exposure to ionizing radiation. *Oncogene* 2003; **22**: 7058–69.

2 Watson GE, Pocock DA, Papworth D, Lorimore SA, Wright EG. *In vivo* chromosomal instability and transmissible aberrations in the progeny of haemopoietic stem cells induced by high- and low-LET radiations. *Int J Radiat Biol* 2001; **77**: 409–17.

3 Bouffler SD, Haines JW, Edwards AA, Harrison JD, Cox R. Lack of detectable transmissible chromosomal instability after *in vivo* or *in vitro* exposure of mouse bone marrow cells to 224Ra alpha particles. *Radiat Res* 2001; **155**: 45–52.

4 Morgan WF. Non-targeted and delayed effects of exposure to ionizing radiation. II. Radiation-induced genomic instability and bystander effects *in vivo*, clastogenic factors and transgenerational effects. *Radiat Res* 2003; **159**: 581–96.

5 Grawe J, Zetterberg G, Amneus H. Flow-cytometric enumeration of

micronucleated polychromatic erythrocytes in mouse peripheral blood. *Cytometry* 1992; **13**: 750–8.
6 Dertinger SD, Torous DK, Tometsko KR. Simple and reliable enumeration of micronucleated reticulocytes with a single-laser flow cytometer. *Mutat Res* 1996; **371**: 283–92.
7 Asano N, Katsuma Y, Tamura H, Higashikuni N, Hayashi M. An automated new technique for scoring the rodent micronucleus assay: computerized image analysis of acridine orange supravitally stained peripheral blood cells. *Mutat Res* 1998; **404**: 149–54.
8 Krzyzanski W, Perez-Ruixo JJ. An assessment of recombinant human erythropoietin effect on reticulocyte production rate and lifespan distribution in healthy subjects. *Pharm Res* 2007; **24**: 758–72.
9 Umeki S, Suzuki T, Kusunoki Y, Seyama T, Fujita S, Kyoizumi S. Development of a mouse model for studying *in vivo* T-cell receptor mutations. *Mutat Res* 1997; **393**: 37–46.
10 Lenarczyk M, Slowikowska MG. The micronucleus assay using peripheral blood reticulocytes from X-ray-exposed mice. *Mutat Res* 1995; **335**: 229–34.
11 Ponnaiya B, Cornforth MN, Ullrich RL. Radiation-induced chromosomal instability in BALB/c and C57BL/6 mice: the difference is as clear as black and white. *Radiat Res* 1997; **147**: 121–5.
12 Goldrath AW, Bevan MJ. Selecting and maintaining a diverse T-cell repertoire. *Nature* 1999; **402**: 255–62.
13 Morley AA. The somatic mutation theory of ageing. *Mutat Res* 1995; **338**: 19–23.
14 Dass SB, Ali SF, Heflich RH, Casciano DA. Frequency of spontaneous and induced micronuclei in the peripheral blood of aging mice. *Mutat Res* 1997; **381**: 105–10.
15 Smith LE, Nagar S, Kim GJ, Morgan WF. Radiation-induced genomic instability: radiation quality and dose response. *Health Phys* 2003; **85**: 23–9.
16 Morgan WF, Sowa MB. Non-targeted bystander effects induced by ionizing radiation. *Mutat Res* 2007; **616**: 159–64.
17 Hayashi T, Morishita Y, Kubo Y *et al.* Long-term effects of radiation dose on inflammatory markers in atomic bomb survivors. *Am J Med* 2005; **118**: 83–6.
18 Yan B, Wang H, Rabbani ZN *et al.* Tumor necrosis factor-alpha is a potent endogenous mutagen that promotes cellular transformation. *Cancer Res* 2006; **66**: 11 565–70.
19 Balmain A, Gray J, Ponder B. The genetics and genomics of cancer. *Nat Genet* 2003; **33** (Suppl): 238–44.
20 Bell DR, Van Zant G. Stem cells, aging, and cancer: inevitabilities and outcomes. *Oncogene* 2004; **23**: 7290–6.
21 Rithidech K, Dunn JJ, Bond VP, Gordon CR, Cronkite EP. Characterization of genetic instability in radiation- and benzene-induced murine acute leukemia. *Mutat Res* 1999; **428**: 33–9.
22 Pierce DA, Shimizu Y, Preston DL, Vaeth M, Mabuchi K. Studies of the mortality of atomic bomb survivors. Report 12, Part I. Cancer: 1950–90. *Radiat Res* 1996; **146**: 1–27.
23 Harada H, Harada Y, Tanaka H, Kimura A, Inaba T. Implications of somatic mutations in the *AML1* gene in radiation-associated and therapy-related myelodysplastic syndrome/acute myeloid leukemia. *Blood* 2003; **101**: 673–80.
24 Kyoizumi S, Kusunoki Y, Hayashi T, Hakoda M, Cologne JB, Nakachi K. Individual variation of somatic gene mutability in relation to cancer susceptibility: prospective study on erythrocyte glycophorin a gene mutations of atomic bomb survivors. *Cancer Res* 2005; **65**: 5462–9.



doi: 10.1111/j.1349-7006.2007.00641.x

RADIATION RESEARCH 168, 1–64 (2007)
0033-7587/07 $15.00


# Solid Cancer Incidence in Atomic Bomb Survivors: 1958–1998

D. L. Preston,[a,1] E. Ron,[b] S. Tokuoka,[c] S. Funamoto,[c] N. Nishi,[c] M. Soda,[c] K. Mabuchi[b] and K. Kodama[c]

[a] *Hirosoft International, Eureka, California;* [b] *Division of Cancer Epidemiology and Genetics, National Cancer Institute, Bethesda, Maryland; and* [c] *Radiation Effects Research Foundation, Hiroshima and Nagasaki, Japan*

## TABLE OF CONTENTS

Preston, D. L., Ron, E., Tokuoka, S., Funamoto, S., Nishi, N., Soda, M., Mabuchi, K. and Kodama, K. Solid Cancer Incidence in Atomic Bomb Survivors: 1958–1998. *Radiat. Res.* 168, 1–64 (2007).

**This is the second general report on radiation effects on the incidence of solid cancers (cancers other than malignancies of the blood or blood-forming organs) among members of the Life Span Study (LSS) cohort of Hiroshima and Nagasaki atomic bomb survivors. The analyses were based on 17,448 first primary cancers (including non-melanoma skin cancer) diagnosed from 1958 through 1998 among 105,427 cohort members with individual dose estimates who were alive and not known to have had cancer prior to 1958. Radiation-associated relative risks and excess rates were considered for all solid cancers as a group, for 19 specific cancer sites or groups of sites, and for five histology groups. Poisson regression methods were used to investigate the magnitude of the radiation-associated risks, the shape of the dose response, how these risks vary with gender, age at exposure, and attained age, and the evidence for inter-site variation in the levels and patterns of the excess risk. For all solid cancers as a group, it was estimated that about 850 (about 11%) of the cases among cohort members with colon doses in excess of 0.005 Gy were associated with atomic bomb radiation exposure. The data were consistent with a linear dose response over the 0- to 2-Gy range, while there was some flattening of the dose response at higher doses. Furthermore, there is a statistically significant dose response when analyses were limited to cohort members with doses of 0.15 Gy or less. The excess risks for all solid cancers as a group and many individual sites exhibit significant variation with gender, attained age, and age at exposure. It was estimated that, at age 70 after exposure at age 30, solid cancer rates increase by about 35% per Gy (90% CI 28%; 43%) for men and 58% per Gy (43%; 69%) for women. For all solid cancers as a group, the excess relative risk (ERR per Gy) decreases by about 17% per decade increase in age at exposure (90% CI 7%; 25%) after allowing for attained-age effects, while the ERR decreased in proportion to attained age to the power 1.65 (90% CI 2.1; 1.2) after allowing for age at exposure. Despite the decline in the ERR with attained age, excess absolute rates appeared to increase throughout the study period, providing further evidence that radiation-associated increases in cancer rates persist throughout life regardless of age at exposure. For all solid cancers as a group, women had somewhat higher excess absolute rates than men (F:M ratio 1.4; 90% CI 1.1; 1.8), but this difference disappears when the analysis was restricted to non-gender-specific cancers. Significant radiation-associated increases in risk were seen for most sites, including oral cavity, esophagus, stomach, colon, liver, lung, non-melanoma skin, breast, ovary, bladder, nervous system and thyroid. Although there was no indication of a statistically significant dose response for cancers of the pancreas, prostate and kidney, the excess relative risks for these sites were also consistent with that for all solid cancers as a group. Dose–response estimates for cancers of the rectum, gallbladder and uterus were not statistically significant, and there were suggestions that the risks for these sites may be lower than those for all solid cancers combined. However, there was emerging evidence from the present data that exposure as a child may increase risks of cancer of the body of the uterus. Elevated risks were seen for all of the five broadly classified histological groups considered, including squamous cell carcinoma, adenocarcinoma, other epithelial cancers, sarcomas and other non-epithelial cancers. Although the data were limited, there was a significant radiation-associated increase in the risk of cancer occurring in adolescence and young adulthood. In view of the persisting increase in solid cancer risks, the LSS should continue to provide important new information on radiation exposure and solid cancer risks for at least another 15 to 20 years.** 

## INTRODUCTION

The Life Span Study (LSS) of atomic bomb survivors continues to provide the best quantitative risk estimates of the carcinogenic effects of low-LET radiation exposure in humans, and it is a major source of epidemiological data used for radiation risk assessment and for establishing radiation protection guidelines. In 1994, the first comprehensive report of cancer incidence in the LSS cohort was published (*1–4*). That report included data for the period of 1958 through 1987. Since then, Pierce and Preston (*5*) evaluated solid cancer incidence through 1994 focusing on the subcohort of about 50,000 LSS survivors who had dose estimates of less than 0.5 Gy to clarify cancer risks at low doses. In addition, results from several studies of cancer incidence for specific sites have been published over the last decades (*6, 17*). These cancer incidence data have added a new dimension to the ongoing series of general reports on cancer and non-cancer mortality in the LSS cohort.

The current report updates the last detailed solid cancer incidence results (*2*) with 11 additional years of follow-up. Cancer incidence data obtained from the Hiroshima and Nagasaki population-based cancer registries assure good ascertainment of malignant tumors and accurate and complete diagnoses, including morphology information and date of diagnosis. The cancer morbidity data permit comprehensive evaluation of radiation risks for both fatal and non-fatal malignancies and risks associated with some histological types of cancer. The accumulating data can also be used to characterize temporal patterns, gender differences, and age-at-exposure effects in the radiation-associated excess risk for a number of cancer sites.

With the follow-up period for these analyses ending in December of 1998, analyses were based on more than 40 years of cancer incidence data for members of the LSS. It should be noted that continued follow-up is important, since 34% of the cancers included in the current analyses were diagnosed during the most recent follow-up period, i.e. 1988–1998. The large number of additional cases provides more stable risk estimates and allows more detailed analyses of effect modification for many types of cancer. Be-

[1] Address for correspondence: Hirosoft International, 1335 H St., Eureka, CA 95501; e-mail: preston@hirosoft.net.

sides extending the follow-up, the present analyses use the newly implemented dosimetry system (DS02) for computing organ dose estimates. DS02 improves on DS86 by refining estimates of the bomb yields and source terms and taking better account of the effects of building and environmental shielding (*18*). The main difference from DS86 is a slight increase in the γ-ray dose estimates for most Hiroshima and Nagasaki survivors and decreases in neutron dose estimates. These changes have little effect on risk estimates (*19*).

The LSS is one of the few radiation effect studies that is comprised of a basically healthy general population, including males and females, exposed to a wide range of radiation doses at all ages. The population was not explicitly selected on the basis of health status at or prior to the time of the bombings; however; to be included in the cohort, people had to have survived for at least 5 years after the bombings. The chance of surviving does depend on various factors including age at the time of exposure and ability to survive the effects (heat, blast and radiation) of the bomb. In the full LSS cohort of 120,321 individuals, about 48% (52% of females and 43% of males) were still alive at the end of 1998. Thus the LSS currently offers a rare opportunity to assess lifetime risks for slightly over 60,000 people. Among survivors exposed to the bombs after age 40, less than 2% were alive at the end of 1998, but what is less appreciated is that slightly over 85% (more than 40,000 people) of the LSS members who were less than 20 years old at the time of the bombings (ATB) were still alive in 1998.

An aspect of the LSS cohort that is often neglected is the highly skewed dose distribution and the large number of survivors who received low-dose, albeit at high dose rate, exposure. Of the 105,000 members of the LSS included in the current analyses, about 35,000 received doses between 5 and 200 mGy. In fact, they comprise about 75% of the cohort members with doses above 5 mGy. This large group of low- to moderate-dose survivors provides adequate statistical power to make direct inferences about cancer risks at low doses (*5*). Although many of the radiation effects observed in the LSS come from survivors with dose estimates in excess of 1 Gy, they comprise less than 3% of the cohort.

The present analyses are based on over 80,000 atomic bomb survivors who were within 10 km of the hypocenter and have DS02 estimated doses, as well as about 25,000 LSS members who were not in Hiroshima or Nagasaki at the time of the bombings. These so-called not-in-city (NIC) LSS members were alive and had a documented permanent residence in either Hiroshima or Nagasaki at the time of the special censuses conducted in 1950–1953. Unlike most recent Life Span Study reports (*1–5, 19–22*), we have included the NIC group to improve the characterization of the LSS cancer background rates, but the analyses include an adjustment to minimize potential bias in radiation risk estimates.

The aim of this report is to further explore the dose–response relationship and the factors that modify that relationship, in particular age and time patterns and the role of gender, and to better characterize risks for individual organs and tissues. With the sizable increase in the number of cancer cases, the report also focuses on describing and interpreting variation in the magnitude and pattern of risks for specific cancer sites compared with those observed for all solid cancers combined. The paper also highlights issues and cancer sites that need clarification and provides suggestions regarding areas for future research.

After a description of the data and methods used in these analyses, we present the results of our analyses of the risks for all solid cancers as a group (page 8) with the primary results summarized in Tables 9 and 10 and Figs. 3 and 4. This section also contains new results on radiation effects on cancer incidence among adolescents and young adults after childhood exposure (page 14). This is followed by presentation of the results of analyses of risks for specific sites (ordered by ICD-O topography codes). Each section contains a short introduction describing differences between baseline rates in Japan and other populations and provides some comments on radiation effects and other environmental risk factors observed in other populations. This is followed by a description of baseline rates in the LSS, with an emphasis on birth cohort effects, and a discussion of the excess risk estimates and effect-modifying factors. Tables 11 and 12 and Figs. 8, 18 and 22 summarize information on levels of risk and effect modification for the sites considered. The Discussion section includes a brief discussion of how risk estimates have changed since the last comprehensive report on solid cancer incidence in the LSS (*2*) (page 48) and our major conclusions (page 55).

## MATERIAL AND METHODS

### *Study Population*

The LSS cohort is comprised of 120,321 people who were selected to include three major groups of registered Hiroshima and Nagasaki residents: (1) atomic bomb survivors who were within 2.5 km of the hypocenter at the time of the bombings (ATB), (2) survivors who were between 2.5 and 10 km of the hypocenter ATB (low- or no-dose group), and (3) residents who were temporarily not in either Hiroshima or Nagasaki or were more than 10 km from the hypocenter in either city (NIC) at the time of the bombings (no-exposure group). The cohort is comprised of about 54,000 survivors in group 1 and 40,000 in group 2 who were living in Hiroshima or Nagasaki in 1950, who responded to a 1950 population census, and for whom there was adequate demographic information for follow-up, as well as 26,580 individuals in group 3 who had returned to Hiroshima or Nagasaki and responded to special A-bomb surveys conducted between 1950 and 1953 concerning location and conditions at the time of the bombings. It is thought that about 100,000 survivors were actually within 2.5-km radius of the hypocenters, which means that the LSS cohort includes about 50% of those survivors and almost all of the survivors who fit the inclusion criteria described above. A sample of the larger number of persons who were 2.5 to 10 km from the hypocenters at the time of the bombs or who were NIC was chosen to match group 1 on age and gender.

NIC cohort members have been followed for cancer incidence and

**TABLE 1**
**Initial Size of the Life Span Study Incidence Cohort[a] and Percentage Surviving[b] by Age at Exposure and Gender**

| Age at exposure | Male | | Female | | Total | |
|---|---|---|---|---|---|---|
| | People | Alive | People | Alive | People | Alive |
| <10 | 11,618 | 89% | 11,917 | 94% | 23,535 | 91% |
| 10–19 | 11,202 | 73% | 14,243 | 87% | 25,445 | 81% |
| 20–29 | 3,686 | 47% | 11,680 | 72% | 15,366 | 66% |
| 30–39 | 5,716 | 17% | 10,928 | 36% | 16,644 | 29% |
| 40–49 | 7,421 | 2% | 9,469 | 5% | 16,890 | 3% |
| ≥50 | 6,237 | 0% | 7,835 | 0% | 14,072 | 0% |
| All ages | 45,880 | 46% | 66,072 | 55% | 111,952 | 52% |

[a] Excludes 96 cohort members with no follow-up data and 8,273 cohort members who died or had been diagnosed with cancer prior to January 1, 1958, but includes 6,525 cohort members without DS02 dose estimates.
[b] As of January 1, 1999.

mortality experience using exactly the same methods as used for the rest of the LSS cohort, so there should be no difference in cancer ascertainment. Because NIC members were matched to survivors on gender and age, their demographic characteristics mirror those of the rest of the cohort. While some earlier analyses suggested that members of the NIC differed from the survivors in the LSS in respect to some socioeconomic indicators and disease rates, more recent analyses of mortality and cancer incidence rate differences between the NIC group and the survivors exposed to negligible doses, i.e. <0.005 Gy, suggest that members of the NIC group are similar to survivors with negligible doses who lived in the urban areas of Hiroshima and Nagasaki (*23*). However, even if disease levels differ somewhat, the NIC group provides useful information on temporal patterns and birth cohort effects. By including an "NIC effect" in the risk models, whatever differences that do exist were not allowed to affect the estimated overall level of radiation risk.

Solid cancer incidence analyses were limited to LSS cohort members who were alive and had not been diagnosed with cancer as of January 1, 1958—the time at which the Hiroshima and Nagasaki population-based tumor registries were established. Since cancer incidence ascertainment is incomplete prior to 1958, it is possible that a small proportion of the early cases were second primary cancers, but this should not have an appreciable effect on the risk estimates.

There were 96 LSS cohort members who could not be traced (48 survivors and 48 people who were not in the city) and 8,273 LSS cohort members (6,988 survivors and 1,285 people who were not in the city) who had died or been diagnosed with cancer before 1958. Thus the solid cancer incidence cohort included 111,952 LSS cohort members. As indicated in Table 1, at the end of follow-up on December 31, 1998, 52% of this group was still alive (55% of the women and 46% of the men).

The higher percentage of surviving females was due in part to the fact that, as in most of the world, women live longer than men and because the initial age distribution of the LSS cohort differed by gender since many men of military age were not in Hiroshima or Nagasaki at the time of the bombings. The gender difference in the percentage of LSS cohort members alive at the end of the current follow-up was largest for individuals who were between the ages of 73 and 82 years at the end of follow-up, i.e. 20–29 years old at the time of the bombings. In this group, 72% of women and only 47% of the men were still alive in 1998. Table 1 also shows that close to 30,000 people had lifetime follow-up. As discussed below, the LSS solid cancer incidence cohort includes 6,525 survivors for whom DS02 doses could not be estimated. Thus the analyses in this report were based on 105,427 (80,180 survivors and 25,247 NIC) eligible LSS cohort members with DS02 dose estimates.

Operation of the Hiroshima and Nagasaki tumor and tissue registries is reviewed regularly by the institutional review boards (IRBs) of the Radiation Effects Research Foundation (RERF) and the registries. Protocols used for vital status and cause of death ascertainment in the Life Span Study are regularly reviewed by the RERF IRB.

### *Cancer Ascertainment and Migration Adjustment*

The Hiroshima and Nagasaki tumor registries were established in 1957 and 1958, respectively. They are managed by RERF and employ active case ascertainment. Cancers are ascertained by RERF abstractors in the large hospitals in Hiroshima city and Nagasaki prefecture. Since most cancer patients in Japan eventually are treated in the large hospitals, few tumors are missed by using this method. For the RERF atomic bomb survivor cohorts, these data are supplemented with information on cancer deaths obtained from death certificates, the Hiroshima and Nagasaki tissue registries (registries of tumor pathology reports and slides), and RERF records from the clinic, autopsy and surgery programs, as well as the RERF leukemia registry. With the approval of the Hiroshima and Nagasaki tumor registries, the RERF cohorts are routinely linked with the registries to identify tumors among cohort members. All computer matches are verified manually (*1*). Tumors were classified and coded according to the guidelines of the International Classification of Diseases for Oncology Version III (ICD-O) (*24*). For this report, information on tumor behavior, topography and morphology, as well as dates and methods of diagnosis, was abstracted from the tumor registries while information on vital status and dates of death was obtained from the LSS mortality follow-up system.

We defined solid cancer cases as all first primary malignant tumors (ICD-O-III codes C00–C89 with behavior code 3, "malignant") (*24*) plus brain and central nervous system tumors of benign and uncertain behavior (ICD codes C70–C72, behavior codes 0, "benign", and 1, "uncertain or unknown nature"), excluding leukemias, lymphomas, myelomas and other lympho-hematopoietic malignancies (ICD-O-II morphology codes 9590–9989). *In situ* cancers (ICDO behavior code 2) were not included in these analyses. As in previous studies of tumor incidence in the LSS (*2, 3, 6–8*), we excluded reported tumors diagnosed outside of the Hiroshima and Nagasaki tumor registries' catchment areas.

Person-years of follow-up were adjusted to reflect immigration and emigration from the tumor registry catchment area. The adjustment involves multiplying the person years in a given gender, birth cohort (age at exposure), time period, and city stratum by an estimate of the probability of residence in the tumor registry catchment area for that stratum. The adjustment factors allow for the fact that some cohort members had left the tumor registry catchment area by 1958 when follow-up for the incidence analyses begins. The residence probability estimates were based on information obtained from Adult Health Study (AHS) cohort records and computed using the methods described in ref. (*25*). Members of the AHS cohort, which is a subset of the LSS, are included in a long-term clinical follow-up study carried out at RERF. Surviving AHS members are contacted once every 2 years, and detailed residence history records are maintained as part of the follow-up process.

Appendix Tables A1 to A19 present case counts and crude rates (cases per 10,000 residence-adjusted person years) stratified by age at exposure (birth cohort), gender and dose. These tables are referenced in the site-specific dose–response sections.

### *Dosimetry*

Individual weighted DS02 organ dose estimates were calculated as the sum of the γ-ray dose plus 10 times the neutron dose. This weighted dose was used to allow for the greater biological effectiveness of neutron doses. Because of the nature of the changes in the new dosimetry, neutrons typically account for a slightly lower proportion of the total DS02 dose estimates than was the case with the DS86 estimates (*18, 19*). For most survivors, neutrons contribute considerably less than 1% of the unweighted total organ dose. In contrast to earlier reports that used units of sievert (Sv) to describe the radiation dose, we use units of gray (Gy) since the dose estimates did not include ICRP tissue weighting factors

and since sieverts are primarily intended to be used for the purposes of radiation protection and not risk estimation (*26, 27*).

Imprecision in the LSS dose estimates results in underestimation of radiation risk and some distortion in the shape of the dose–response curve. To adjust for the impact of bias arising as a result of random errors in individual dose estimates, shielded kerma estimates above 4 Gy were truncated to 4 Gy, and DS02 estimates were replaced by expected survivor dose estimates using the method developed by Pierce *et al.* (*28*). As in other recent analyses, we assumed 35% errors in individual DS02 dose estimates. These adjustments produce bias-corrected risk estimates and increase estimates of the slope of the dose response by about 10% in linear models.

Information on exact location and shielding conditions is insufficient to allow the computation of DS02 dose estimates for 6,525 proximally exposed cohort members (survivors who were within 3 km of the hypocenter) who otherwise met the eligibility requirements for inclusion in the cancer incidence study population. These cohort members were excluded from the analyses. As discussed in ref. (*29*), various methods were used to impute doses for cohort members at greater distances with limited shielding information. The weighted colon doses for survivors at these distances are less than 6 mGy.

*Statistical Analysis and Organization of the Data for Analysis*

The aim of these statistical analyses was to describe cancer incidence rates as functions of dose, age, gender, age at exposure, birth cohort, city and other factors. The primary data for these analyses consist of a table of case counts and person-years cross-classified by city, gender, radiation dose to the colon (22 categories, as described below, and an unknown category), follow-up period (10 categories with cutpoints on January 1 of 1961, 1966, 1971, 1976, 1981, 1986, 1988, 1991 and 1996), attained age (17 5-year categories from ages 5 through 84 and 85 or more), age at exposure (14 5-year categories for ages 0 through 69 and 70 or more), and distance from the hypocenter (within 3 km, 3–10 km, and NIC). Dose categories were defined in terms of weighted DS02 colon dose estimates (described above). The dose category cutpoints were 0.005, 0.02, 0.04, 0.06, 0.08, 0.1, 0.125, 0.15, 0.175, 0.20, 0.25, 0.30, 0.50, 0.75, 1.0, 1.25, 1.5, 1.75, 2.0, 2.5 and 3.0 Gy. The analysis table has about 27,000 cells with some person years at risk, each of which contains cause-specific counts of the number of cases and person-years along with mean values of age, age at exposure, year and weighted organ doses. This data set along with program and log files used for the basic models discussed in this report are available from the RERF website (www.rerf.or.jp). Analyses for all solid cancers as a group were based on colon doses, while analyses of specific sites use the dose to the tissue deemed most relevant for that site. We distinguished between in-city and NIC cohort members in the baseline rate models. The in-city group included survivors who were within 10 km of the hypocenter at the time of the bombings. Proximal survivors received doses ranging from less than 1 mGy to several Gy depending on location and shielding. Within this group the mean estimated doses tend to double with each 200-m decrease in distance from the hypocenter. Cohort members who were between 3 and 10 km from the hypocenter at the time of the bombings (distal survivors) received negligible radiation exposures from the bombs, and their doses were taken as 0. While proximal survivors provided some information on baseline rates, cancer rates for the distal survivors are a primary source of information on the level of the baseline rates in this population. The NIC group included people who were not in the cities (i.e. at least 10 km from the hypocenter) at the time of the bombing. Dose estimates were taken as zero for members of the NIC group. Since the background rate models were stratified on presence in the city, the NIC group did not contribute to estimation of the level of the baseline rates but did provide information on the variation of these rates with gender, birth cohort, and attained age. In analyses of thyroid and non-melanoma skin cancers, the rate table was also stratified on participation in the Adult Health Study. This more detailed rate table has about 45,000 cells.

Poisson regression methods for rates (*30, 31*) were used to develop descriptive models for cancer incidence rates and to characterize radiation effects on these rates. Aside from the grouping of persons on dose and age-at-exposure categories, these methods are equivalent to analysis of survival times under the approximation that the rates are piecewise constant in age within cells of the summary table. Parameter estimation and inference were carried out using the Epicure software (*32*). Significance tests and confidence bounds were based on $\chi^2$ approximations to the distribution of likelihood ratio tests.

We made use of general rate (hazard) models for both the ERR and the EAR. An ERR model has the form

$$\lambda_0(c, s, a, b, l)[1 + ERR(d, e, s, a)],$$

where $\lambda_0(\cdot)$ is the baseline, or background, cancer incidence rate (i.e. the rate for people with zero dose) and the function $ERR(d, e, s, a)$ describes the relative change in rates associated with dose $d$ allowing for effects of age at exposure ($e$), gender ($s$), and attained age ($a$). In an EAR model, we describe the absolute difference between the rates among those exposed to dose $d$ and the rates among those exposed to zero dose. The general form of an EAR model is

$$\lambda_0\ (c,s,a,b,l) + EAR(d,e,s,a).$$

The background rate was taken to depend on attained age ($a$), year of birth ($b$), gender ($s$), city ($c$), and location at the time of the bombing ($l$). In this report we used parametric models for the background rates as described below.

The ERR and EAR functions are described as parametric functions of the form $\rho(d)\varepsilon(e, s, a)$ in which $\rho(d)$ describes the shape of the dose–response function and $\varepsilon(e, s, a)$ describes risk variation with gender, time or other factors (such as participation in AHS examinations). In addition to the linear dose response [$\rho(d) = \beta d$], we considered alternative dose–response models in these analyses including

$$\rho(d) = \beta d + \gamma d^2 \qquad \text{Linear–quadratic}$$

$$\rho(d) = \gamma d^2 \qquad \text{Quadratic}$$

$$\rho(d) = \begin{cases} \beta(d - d_t) & d > d_t \\ 0 & d \le d_t \end{cases} \qquad \text{Linear threshold}$$

$$\rho(d) = \delta_j \qquad d_{j-1} \le d < d_j \qquad \text{"Nonparametric"}$$

The dose–response parameters were not constrained to be positive. The primary test for non-linearity was based on comparison of linear and linear-quadratic dose–response models. For linear-quadratic models, we describe the curvature of the model using the ratio of the coefficient of quadratic term to that of the linear term. That is, curvature is defined as $\gamma/\beta$. Risk estimates for the linear model were based on fits to all of the data (i.e. for cohort members with dose estimates) using the adjusted and truncated doses described above. However, because of concerns about flattening of the dose response at high doses (which were apparent in the all-solid cancer dose response and may reflect cell killing effects or effects of dose error not accounted for by the dose adjustments used), tests for non-linearity were based on a model in which the dose response was taken as linear-quadratic in the 0–2-Gy dose range but was allowed to have a different slope (with no continuity constraint) at higher doses. This was done because a primary reason for the consideration of non-linear models concerns the possible lack of linearity at low doses, and we did not want to bias estimates of the curvature at low doses due to the influence of high dose data.

The "nonparametric" specification above is useful for qualitative assessment of the nature of the dose response. To minimize the effect of an arbitrary choice of dose categories, we used the large number of dose categories in the analysis table and then smoothed the resulting parameter estimates $\delta_j$, which were individually quite imprecise due to the narrow width of dose categories. The smoothing method was a locally weighted linear regression described in ref. (*5*), with weights defined as the product of a smoothing weight and the precision (inverse variance) of the estimates $\delta_j$.

Effect modification was generally described using multiplicative models such as

$$\varepsilon(e, s, a) = \theta_s \exp\{\alpha e + \omega \log(a)\}, \quad (1)$$

which we note applies equally to all dose levels. As a convention, of no real consequence, we parameterize the effect modification model so that $\rho(d)$ corresponds to the dose response, averaged over gender (where appropriate), for $e = 30$, $a = 70$, which we call the standardized ERR or EAR. In some cases these excess risk models were extended to include AHS participation effects. In these analyses $\rho(d)$ corresponds to the excess risk for a cohort member who has not participated in any AHS examinations. EAR estimates are given in units of excess cases per 10,000 PY at 1 Gy. For all solid cancers as a group and some individual sites, we considered extensions of the model (1) in which the effects of age at exposure or attained age on the excess risk were not constrained to be monotonic. In particular we added quadratic or quadratic spline terms in age or age at exposure and also considered non-parametric descriptions that involved categorical age-at-exposure effects.

For sites with small numbers of radiation-associated cases, it was not feasible to fit relatively detailed effect modification models like that described in Eq. (1). Therefore, for sites with less than 35 radiation-associated cases, the results were based on simple time-constant ERR or EAR models with no modifying effects of gender, attained age, age at exposure or other factors. In these cases, we described possible effect modification based on $P$ values of score tests for specific parameters of interest.

It the text, we refer to risk models in which we estimate effect modification parameters as the standard or full models, whereas risk models without effect modification parameters are referred to as simple or time-constant excess risk models.

Gender-specific parametric models for the background rates $\lambda_0(\cdot)$ were used in most analyses. In the most general models, for each gender, the log rate was described using city and exposure status effects together with piecewise quadratic functions of log age joining smoothly at ages 40 and 70 and piecewise quadratic functions of birth year joining smoothly at 1915 (age at exposure 30) and 1895 (age at exposure 50). A smooth piecewise quadratic function of $x$ with join points at $x_1$ and $x_2$ can be written as $\beta_0 + \beta_1 x + \beta_2 x^2 + \beta_3 \max(x - x_1, 0)^2 + \beta_4 \max(x - x_2, 0)^2$. This parameterization provides a flexible but relatively parsimonious description in which city, exposure status, and birth cohort have multiplicative effects on the rates.

In describing the patterns in the baseline rates, we often summarize the dependence on attained age by reporting that the increase in rate is proportional to some power of age. This summary was obtained by fitting a slightly simpler model in which the log baseline rates was taken to be linear in attained age. Since background rates allowed for age, gender, city and birth cohort effects, the excess risk estimates are termed adjusted ERR or EAR estimates.

As explained in LSS Report 13 (*20*), interpretation and generalization of gender and age-at-exposure effects on LSS excess risks depends on the nature of gender and birth cohort effects on background rates. Therefore, for all solid cancers and the more common cancer sites, we briefly describe how background rates vary with gender and birth cohort. Birth cohort effects are summarized in terms of the percentage change in the estimated background rate for a 70-year-old relative to that for a person of the same age who was born in 1915.

Since all members of this cohort were exposed at the same time, birth cohort and age at exposure are perfectly correlated. Thus comparison of variation in age-specific background rates with birth cohort to variation in the radiation effect with age at exposure for the ERR and EAR may provide insights into the interpretation of age-at-exposure effects. For example, if the EAR does not depend on age at exposure and baseline rates are increasing (decreasing) with birth cohort, then the ERR must decrease (increase) with age at exposure. In this case, we could say that radiation appears to act additively with respect to the factors responsible for birth cohort variation in baseline rates. Conversely, if the ERR does not vary with age at exposure and there is a birth cohort effect on the baseline rate, then the age-at-exposure effect on the EAR should parallel the birth cohort effect on the baseline rates, and we could say that radiation tends to act multiplicatively with respect to the factors responsible for the birth cohort effect. Such patterns could arise by chance, but this seems rather unlikely.

In presenting results for sites for which the estimated number of radiation-associated cancer cases is more than 20, we used plots to describe the fitted dose response and illustrate the age and age-at-exposure dependence of the excess risk. To illustrate the dose response and summarize the uncertainty in this response, we present plots of the fitted linear ERR along with smoothed and unsmoothed non-parametric ERR estimates and plus or minus one standard error bounds for the smoothed estimate. The dose–response curves in these plots are based on cohort members with estimated doses of 2 Gy or less, averaged over gender and standardized to diagnosis at age 70 after exposure at age 30.

The plots used to summarize age and age-at-exposure variation in the excess risk present gender-averaged ERR or EAR risk estimates at 1 Gy for three ages at exposure (10, 30 and 50 years old) as a function of age at diagnosis (attained age). The fitted curves were based on simple parametric effect modification models of the form given in Eq. (1).

As noted above, comparison of variation in age-specific baseline rates with birth cohort and variation in the radiation-associated excess rate with age-at-exposure may lead to useful insights regarding interpretation of age-at-exposure effects. To examine this, we present plots that contrast variation in age-specific baseline rates (relative to people born in 1915) to variation in the ERR or EAR relative to people who were age 30 at exposure for some sites.

## RESULTS

Among the 105,427 members of the LSS cohort included in this study, 17,448 first primary solid cancers were diagnosed from 1958–1998 (Table 2). This included 3,994 cases among the NIC members, a group that had been excluded in most earlier reports (*2, 20, 21*). About 34% ($n$ = 5,956) of the cases occurred in the 11 years (1988–1998) since the last comprehensive incidence report (*2*). Of these new cases, 4,538 occurred among cohort members who were in the cities at the time of the bombing and 1,418 cases occurred among members of the NIC group. Recent case-finding efforts also identified an additional 305 cases that occurred among in-city cohort members for the period 1958–1987 but were not included in the previous report.

Stomach cancer was the most common cancer in the cohort, accounting for more than 25% of all cases (Table 2). Other commonly occurring cancers include lung (10%), liver (9%), colon (9%), rectum (5%), female breast (6%), and cervix (5%). This distribution was similar to what would be expected in Japan for this period (*33*). Table 3 also shows that, in this cohort, 54% of all cancers occurred among women. Cancer of the gallbladder, non-melanoma skin, brain and nervous system, and thyroid were particularly more frequent (>60%) among women. The mean age at diagnosis varied somewhat, with breast and thyroid cancers having the lowest mean age and cancers of the gallbladder, pancreas, lung, non-melanoma skin, prostate and bladder having mean ages over 70 years.

Of the cancers used in this analysis 13,784 (79%) were verified histologically, 1,636 (9%) were diagnosed based on direct observation during procedures such as endoscopy, bronchoscopy or surgery and 391 (2%) were based on clin-

**TABLE 2**
**Solid Cancer Cases[a] in the Life Span Study, 1958–1998**

| Site | Dose (categories of weighted organ dose in Gy)[b] | | | | | |
|---|---|---|---|---|---|---|
| | NIC | <0.005 | −0.5 | −1 | 1–4 | Total |
| All solid cancers | 3,994 | 5,603 | 6,479 | 649 | 723 | 17,448 |
| Oral cavity and pharynx | 61 | 91 | 94 | 12 | 19 | 277 |
| Tongue | 22 | 28 | 30 | 3 | 4 | 87 |
| Salivary gland | 7 | 12 | 14 | 2 | 7 | 42 |
| Lip | 0 | 1 | 3 | 0 | 0 | 4 |
| Mouth | 17 | 25 | 21 | 3 | 6 | 72 |
| Pharynx | 15 | 25 | 26 | 4 | 2 | 72 |
| Digestive system | 2,368 | 3,269 | 3,740 | 355 | 320 | 10,052 |
| Esophagus | 84 | 116 | 127 | 11 | 14 | 352 |
| Stomach | 1,128 | 1,507 | 1,785 | 158 | 152 | 4,730 |
| Colon | 351 | 494 | 560 | 53 | 58 | 1,516 |
| Rectum | 187 | 275 | 323 | 30 | 23 | 838 |
| Liver | 348 | 501 | 539 | 61 | 45 | 1,494 |
| Gallbladder | 134 | 197 | 193 | 16 | 9 | 549 |
| Pancreas | 121 | 162 | 190 | 25 | 14 | 512 |
| Other digestive | 15 | 17 | 23 | 1 | 5 | 61 |
| Respiratory system | 456 | 640 | 738 | 75 | 92 | 2,001 |
| Nasal cavity | 17 | 25 | 32 | 4 | 4 | 82 |
| Larynx | 23 | 46 | 56 | 6 | 2 | 133 |
| Lung | 415 | 555 | 641 | 64 | 84 | 1,759 |
| Other respiratory | 1 | 14 | 9 | 1 | 2 | 27 |
| Skin, bone or connective tissues | 70 | 136 | 127 | 18 | 49 | 400 |
| Bone | 1 | 12 | 3 | 0 | 4 | 20 |
| Connective tissue | 10 | 10 | 9 | 2 | 2 | 33 |
| Non-melanoma skin cancer | 55 | 108 | 110 | 15 | 42 | 330 |
| Melanoma | 4 | 6 | 5 | 1 | 1 | 17 |
| Breast | 228 | 321 | 381 | 54 | 98 | 1,082 |
| Female breast | 226 | 320 | 377 | 53 | 97 | 1,073 |
| Male breast | 2 | 1 | 4 | 1 | 1 | 9 |
| Female genital | 348 | 476 | 559 | 40 | 34 | 1,457 |
| Cervix | 214 | 275 | 328 | 26 | 16 | 859 |
| Uterine corpus | 48 | 62 | 64 | 4 | 6 | 184 |
| Uterus, NOS | 25 | 34 | 58 | 0 | 2 | 119 |
| Ovary | 55 | 87 | 84 | 9 | 10 | 245 |
| Other female genital | 6 | 18 | 25 | 1 | 0 | 50 |
| Male genital | 115 | 135 | 145 | 14 | 11 | 420 |
| Prostate | 106 | 125 | 134 | 13 | 9 | 387 |
| Testicular | 4 | 3 | 8 | 1 | 1 | 17 |
| Other male genital | 5 | 7 | 3 | 0 | 1 | 16 |
| Urinary system | 173 | 224 | 278 | 31 | 35 | 741 |
| Bladder | 117 | 130 | 182 | 20 | 20 | 469 |
| Renal cell | 37 | 60 | 61 | 3 | 6 | 167 |
| Renal pelvis | 16 | 26 | 30 | 5 | 3 | 80 |
| Other urinary | 3 | 8 | 5 | 3 | 6 | 25 |
| Brain and central nervous system | 40 | 104 | 106 | 15 | 16 | 281 |
| Brain, malignant | 15 | 24 | 18 | 4 | 3 | 64 |
| Brain, benign | 4 | 10 | 14 | 1 | 0 | 29 |
| Other CNS, malignant | 0 | 6 | 3 | 2 | 1 | 12 |
| Other CNS, benign | 21 | 64 | 71 | 8 | 12 | 176 |
| Thyroid | 70 | 136 | 202 | 24 | 39 | 471 |
| Other solid cancers | 65 | 71 | 109 | 11 | 10 | 266 |

[a] All first primary malignant tumors (ICD-O-III codes C00–C89, behavior code 3), excluding leukemia, lymphoma, myeloma and other lympho-hematopoietic malignancies, plus brain and central nervous system tumors of benign, uncertain or unknown behavior (ICD-O-III codes C70–C72, behavior codes 0 and 1).

[b] Dose categories for specific sites were defined in terms of the weighted organ dose used in analyses of that site. Case counts for all solid cancers and other groups of sites are the sum of the case counts in this table.

ical diagnoses only; for 1,616 cases (9%) the diagnosis was based solely on death certificate data. Less than 4% of the cases were identified only from autopsy records. As indicated in Table 3, the percentage of histologically confirmed tumors varied widely by site and was 90% or higher for cancers of the oral cavity, colon, rectum, non-melanoma skin cancer, breast, uterine corpus, cervix and thyroid. In contrast, it was less than 60% for cancers of the liver, pan-

**TABLE 3**
**Solid Cancer Case Summary Information: Percentage of Cases among Women, Mean Age at Diagnosis, Histological Confirmation and Death-Certificate-Only Rates by Site, 1958–1998**

| Site | Percentage female | Mean age at diagnosis | Histological confirmation | Death certificate only |
|---|---|---|---|---|
| All solid cancers | 54 | 67.4 | 79% | 9% |
| Oral cavity and pharynx | 40 | 63.5 | 95% | 3% |
| Esophagus | 19 | 69.0 | 80% | 7% |
| Stomach | 46 | 67.7 | 80% | 10% |
| Colon | 54 | 69.3 | 90% | 5% |
| Rectum | 50 | 68.0 | 90% | 5% |
| Liver | 40 | 67.0 | 41% | 21% |
| Gallbladder | 67 | 71.9 | 65% | 12% |
| Pancreas | 56 | 71.4 | 52% | 20% |
| Lung | 41 | 71.2 | 73% | 15% |
| Non-melanoma skin | 63 | 72.4 | 97% | 2% |
| Female breast | 100 | 59.8 | 95% | 1% |
| Uterine corpus | 100 | 60.9 | 97% | 1% |
| Cervix | 100 | 60.0 | 97% | 1% |
| Uterus, NOS | 100 | 60.9 | 55% | 30% |
| Ovary | 100 | 63.7 | 88% | 5% |
| Prostate | 0 | 76.1 | 88% | 5% |
| Bladder | 33 | 70.6 | 88% | 5% |
| Renal cell | 46 | 67.9 | 82% | 7% |
| Brain and CNS | 67 | 62.6 | 81% | 6% |
| Thyroid | 81 | 60.4 | 95% | 1% |
| Other solid cancers[a] | 50 | 68.2 | 75% | 13% |

[a] Solid cancers not included in any of the above groups.

creas, and uterus NOS. The proportion of death certificate only (DCO) exceeded 15% for cancers of the liver, pancreas, lung and uterus NOS.

After allowing for migration effects, there were almost 2.8 million person-years of follow-up, or an average of 26.2 years per person over the 41-year follow-up period. Table 4 provides information on the distribution of solid cancer cases, migration-adjusted person-years, and subjects for the solid cancer incidence cohort.

For most of the sites or groups of sites considered in these analyses, we described recent world-population age-standardized incidence rates for Japan as presented in ref. (*33*). For comparison, we present world-population age-standardized rates from the U.S. SEER registry program, the Swedish national cancer registry, and the cancer registry for Cali, Colombia (*34*) in Table 5. The world standard population used and the computation of standardized rates is described in ref. (*34*).

Comparison of the rates from these populations highlights the marked differences for some cancers: For example, stomach and liver cancer rates in Japan are several times those in the other populations, while prostate cancer rates in Japan are lower than those in the other countries. This striking inter-population variation in baseline rates for some sites raises difficult but important questions about how LSS-based risk estimates should be used to assess risks in other populations. These issues, which are quite important for radiation protection but are beyond the scope of this paper, are discussed elsewhere (*26, 35–37*).

In Japan, as in other countries, cancer incidence rates have been changing over time. Table 6 provides information on temporal changes in Japanese solid cancer incidence rates from 1975 to 1999 for most of the sites considered in this report. These rates are based on data from several Japanese cancer registries (including the Hiroshima and Nagasaki registries) (*33*).

The most striking declines were seen for stomach and cervical cancers, while age-standardized rates for most other sites and for all solid cancers as a group increased over this 25-year period.

### *Solid Cancer*

#### *1. Baseline rates and birth cohort effects*

Throughout much of life, the baseline solid cancer rates for men and women in the LSS increase roughly in proportion to attained age to the power 5.5 with an apparent downturn in the rates at ages of around 90. The downturn was more pronounced for men than for women.

Examination of baseline solid cancer incidence rates in the LSS indicated that age-specific cancer rates had increased with the passage of time and that this increase was larger in men than in women. Estimates of the gender-specific change in age-specific rates relative to those for people born in 1915 are shown in Fig. 1.

Age-specific rates for the 1900 birth cohort were 25% lower for men and 10% lower for women than those for the 1915 birth cohort, and the rates for the 1935 birth cohort

**TABLE 4**
**Solid Cancers, Person Years of Follow-up, and Number of LSS Cohort Members[a] by Gender, City, Age at Exposure and Dose, 1958–1998**

| | Male | | | Female | | | Total | | |
|---|---|---|---|---|---|---|---|---|---|
| | Solid cancers | Person years | People | Solid cancers | Person years | People | Solid cancers | Person years | People |
| Total | 7,969 | 1,040,278 | 42,902 | 9,479 | 1,724,452 | 62,525 | 17,448 | 2,764,730 | 105,427 |
| City | | | | | | | | | |
| Hiroshima | 5,887 | 733,073 | 29,520 | 7,044 | 1,234,528 | 43,910 | 12,931 | 1,967,601 | 73,430 |
| Nagasaki | 2,082 | 307,205 | 13,382 | 2,435 | 489,924 | 18,615 | 4,517 | 797,129 | 31,997 |
| Age at exposure | | | | | | | | | |
| 0–9 | 658 | 327,811 | 11,199 | 664 | 352,479 | 11,482 | 1,322 | 680,290 | 22,681 |
| 10–19 | 1,751 | 304,530 | 10,372 | 1,522 | 402,908 | 12,687 | 3,273 | 707,438 | 23,059 |
| 20–29 | 935 | 98,569 | 3,301 | 2,025 | 364,049 | 10,965 | 2,960 | 462,618 | 14,266 |
| 30–39 | 1,634 | 130,949 | 5,221 | 2,398 | 315,402 | 10,596 | 4,032 | 446,351 | 15,817 |
| 40–49 | 1,883 | 121,240 | 6,912 | 1,877 | 202,004 | 9,166 | 3,760 | 323,244 | 16,078 |
| 50+ | 1,108 | 57,179 | 5,897 | 993 | 87,610 | 7,629 | 2,101 | 144,789 | 13,526 |
| Weighted colon dose (Gy) | | | | | | | | | |
| NIC | 1,962 | 261,594 | 10,491 | 2,032 | 419,150 | 14,756 | 3,994 | 680,744 | 25,247 |
| <0.005 | 2,574 | 342,504 | 14,418 | 3,029 | 575,695 | 21,127 | 5,603 | 918,199 | 35,545 |
| −0.1 | 1,961 | 275,110 | 11,260 | 2,445 | 454,493 | 16,529 | 4,406 | 729,603 | 27,789 |
| −0.2 | 390 | 52,924 | 2,150 | 578 | 93,001 | 3,377 | 968 | 145,925 | 5,527 |
| −0.5 | 484 | 54,819 | 2,284 | 660 | 99,067 | 3,651 | 1,144 | 153,886 | 5,935 |
| −1 | 304 | 29,615 | 1,285 | 384 | 51,636 | 1,888 | 688 | 81,251 | 3,173 |
| −2 | 211 | 17,593 | 746 | 249 | 23,819 | 901 | 460 | 41,412 | 1,647 |
| −2–4 | 83 | 6,120 | 268 | 102 | 7,591 | 296 | 185 | 13,711 | 564 |

[a] Excludes 96 cohort members with no follow-up data, 8,273 cohort members who died or had been diagnosed with cancer prior to January 1, 1958, and 6,525 cohort members for whom DS02 dose estimates could not be computed.

**TABLE 5**
**Comparison of World-Population Age-Standardized Incidence Rates per 100,000 People for Selected Solid Cancers in Japan, the United States, Colombia and Sweden**

| | | Japan[a] (1995–1999) | | SEER (1993–1997) | | Colombia, Cali (1992–1996) | | Sweden (1993–1997) | |
|---|---|---|---|---|---|---|---|---|---|
| Site | ICD-10 | Male | Female | Male | Female | Male | Female | Male | Female |
| All solid cancers | C00–C89 | 271.1 | 168.6 | 335.8 | 257.6 | 173.8 | 184.2 | 233.2 | 224.9 |
| Oral cavity | C00–C14 | 6.2 | 2.0 | 12.3 | 4.7 | 6.0 | 4.1 | 6.8 | 3.1 |
| Esophagus | C15 | 11.0 | 1.6 | 5.1 | 1.4 | 3.9 | 1.8 | 3.1 | 0.9 |
| Stomach | C16 | 61.8 | 23.8 | 7.7 | 3.2 | 30.5 | 18.8 | 8.6 | 4.4 |
| Colon | C18 | 31.2 | 18.5 | 25.9 | 19.8 | 7.2 | 8.4 | 17.7 | 15.0 |
| Rectum[b] | C19–20 | 18.7 | 8.7 | 12.3 | 7.3 | 4.6 | 4.3 | 12.2 | 7.6 |
| Liver | C22 | 23.5 | 7.5 | 4.9 | 1.8 | 3.0 | 2.5 | 4.1 | 2.3 |
| Gallbladder | C23–24 | 6.7 | 5.0 | 1.5 | 1.5 | 2.6 | 6.6 | 2.0 | 3.0 |
| Pancreas | C25 | 9.0 | 5.2 | 7.7 | 5.7 | 4.6 | 4.4 | 6.3 | 5.3 |
| Lung | C33–34 | 37.6 | 11.8 | 55.7 | 33.5 | 22.3 | 9.5 | 22.0 | 12.9 |
| Breast[c] | C50 | | 36.0 | 0.7 | 89.5 | 0.1 | 37.3 | 0.4 | 76.5 |
| Cervix | C53 | | 6.6 | | 7.4 | | 29.8 | | 7.7 |
| Uterine corpus | C54 | | 5.4 | | 17.6 | | 5.9 | | 14.3 |
| Uterus, NOS | C55 | | 0.8 | | 0.3 | | 0.9 | | 1.2 |
| Ovary | C56 | | 7.0 | | 12.5 | | 10.1 | | 15.2 |
| Prostate | C61 | 14.1 | | 112.2 | | 42.2 | | 63.0 | |
| Kidney[d] | C64 | 6.4 | 2.5 | 9.6 | 4.9 | 2.9 | 2.3 | 7.8 | 4.8 |
| Bladder | C67 | 9.7 | 2.2 | 21.5 | 5.8 | 6.1 | 2.1 | 17.8 | 4.8 |
| Brain, CNS | C70–72 | 2.7 | 2.0 | 6.5 | 4.4 | 5.0 | 3.6 | 6.6 | 4.7 |
| Thyroid | C73 | 1.6 | 6.6 | 2.7 | 7.5 | 1.6 | 6.7 | 1.3 | 3.5 |
| Other solid cancers | | 30.9 | 20.8 | 49.5 | 28.8 | 31.2 | 25.1 | 53.5 | 37.7 |

[a] Japanese rates taken from (34) while all data for other countries are from *Cancer Incidence in Five Continents, VIII* (*35*).

[b] Japanese rates include anus (C21).

[c] Japanese rates do not include male breast cancer rates.

[d] Japanese rates include renal pelvis (C65), ureter (C66), and other urinary organs (C68).

were predicted to be about 50% greater for males and 20% greater for females than those for people born in 1915. If these trends continue, cancer rates would be about 70% higher for men and 40% higher for women belonging to the 1945 birth cohort. The patterns of change in baseline rates over time differed for specific cancer sites, so they are described in the sections presenting results for each cancer site.

As illustrated in the left panel of Fig. 2, the male:female cancer incidence ratio at age 70 years was about 2.1 for people born in 1900 and increased to about 2.6 for people born in 1925. The current data suggest that for people born in 1935, the gender ratio will be about 2.9 when they reach age 70.

The right panel in Fig. 2 also illustrates the male:female background ratio as a function of age for people born in 1915. Gender ratios are shown with and without the inclusion of gender-specific cancers (breast, prostate and cancers of male or female genital organs). In general, men had lower cancer rates than women until about age 50, after which men had higher rates when all cancers were considered. Excluding gender-specific cancers, cancer rates were higher for men starting at around age 35 years. After age 65, when rates were the highest, the male:female ratio was similar whether or not gender-specific cancers were included. Understanding gender differences in the baseline rates is important to interpretation of gender differences in radiation effects on the ERR.

### 2. *Dose response and effect modification*

Table 7 presents the crude incidence rates for solid cancers. The rates suggested a dose response for men and women at all ages at exposure.

The crude rates were higher for men than women in almost all dose and age-at-exposure categories. As seen in Table 8, the crude relative risks plainly pointed to a dose–response relationship for each of the six age-at-exposure groups and both sexes. Relative risks appeared to be greater for persons exposed to the bombs relatively early in life and for females.

Based on the standard linear ERR model with effect modification in which age, year of birth, gender, city of the bombing, and exposure status (in-city, not-in-city) were included in the background, there was clear evidence of a dose response. The model predicted that about 853 excess cancers occurred between 1958 and 1998 among LSS survivors exposed to ≥0.005 Gy (Table 9).

Among these survivors about 11% of the solid cancers were attributable to radiation exposure, but about 48% (307 of the 645) of the cancers among survivors having doses of at least 1 Gy were attributable to radiation exposure (Table 9). About 156 (18%) of the estimated excess cancers occurred among individuals in the low to moderate dose range of 5–200 mGy. The attributable fraction was 13% for females and 8% for males, and it decreased with increasing age at exposure or age at diagnosis. Among those exposed to at least 0.005 Gy, the attributable fractions were 20%, 18%, 10% and 6% for age-at-exposure groups of 0–9, 10–19, 20–39 and 40+ years, respectively. Among people who received at least 0.005 Gy, attributable fractions were 34%, 17%, 9% and 5% in age-at-diagnosis groups of 0–39, 40–59, 60–79 and 80+ years, respectively.

Figure 3 provides a summary of the solid cancer dose response. The solid line indicates the fitted linear dose response determined using the data in the 0- to 2-Gy range. The dashed line represents the smoothed non-parametric dose–response function and the dotted lines the uncertainty (plus or minus one standard error) in the non-parametric smoothed dose response. The circles indicate the ERR at the mean dose in each of 22 specific dose categories. It can be seen that the linear dose response fit the data well. There was no significant linear-quadratic non-linearity in the dose response over the 0- to 2-Gy dose range ($P = 0.09$). The estimated curvature was 0.3 (90% CI 0.01; 0.90). As noted in the Material and Methods section, the curvature of a linear-quadratic dose–response model is defined as the ratio of the parameter associated with dose-squared to the parameter for dose. There was a statistically significant dose response in the range of 0–0.15 Gy ($P = 0.06$), and the trend in this low-dose range was consistent with that for the full dose range ($P > 0.5$). Based on fitting a series of models with thresholds at the dose cutpoints in the person-year table, the best estimate of a threshold was 0.04 Gy with an upper 90% confidence bound of about 0.085 Gy. However, this model did not fit significantly better than a linear model.

Parameter estimates for fitted ERR and EAR linear dose–response models with effect modification by age at exposure, attained age, and gender are presented in the upper portion of Table 10. In these models, a common linear dose response was assumed over the full range (0–4 Gy) of doses.

For a person aged 70 who was exposed to the bombings at age 30, the gender-averaged estimate of the excess ERR per Gy ($ERR_{1Gy}$) was 0.47 for all solid cancers combined with a 90% confidence interval of 0.40 to 0.54. Based on a linear model, this would mean that solid cancer risks are increased by about 10% for LSS survivors exposed to over 0.005 Gy for whom the mean weighted colon dose is 0.23 Gy. The $ERR_{1Gy}$ was 60% higher for women (0.58) than men (0.35).

The solid cancer ERR varied significantly with both age at exposure and attained age. Figure 4 illustrates the temporal patterns in the gender-averaged ERR (left panel) and EAR (right panel) solid cancer estimates by attained age for various ages at exposure.

The ERR decreased in proportion to attained age to the power −1.65 for any age at exposure. The attained-age-specific ERR decreased by about 17% per decade increase in age at exposure, so that the ERR for someone age 10 at